DoE Award Number: DE-FE0003892

Multiscale Modeling of Grain Boundary Segregation and Embrittlement in Tungsten for Mechanistic Design of Alloys for Coal Fired Plants

Jian Luo, Naixie Zhou, Zhao Zhang & Mojtaba Samiee
University of California, San Diego & Clemson University

Vikas Tomar, Hongsuk Lee & Niranjan Parab
School of Aeronautics and Astronautics, Purdue University

Program Manager: Dr. Richard Dunst

June 11, 2013

This UCR Project

GB = Grain Boundary

Using tungsten (W) based binary & ternary alloys as model systems…

Develop thermodynamic theories and models to predict a "new" type of high-T (premelting-like) GB segregation

Luo *et al.* at Clemson/UCSD

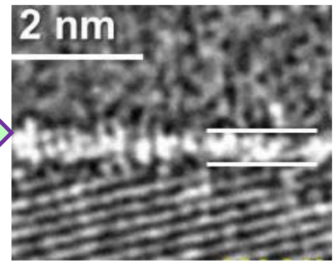

Develop multiscale modeling strategies to link GB segregation with GB embrittlement

Tomar *et al.* at Purdue

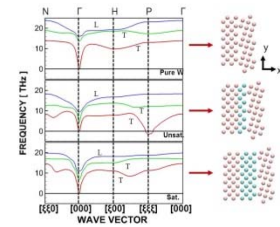

Phonon Dispersion

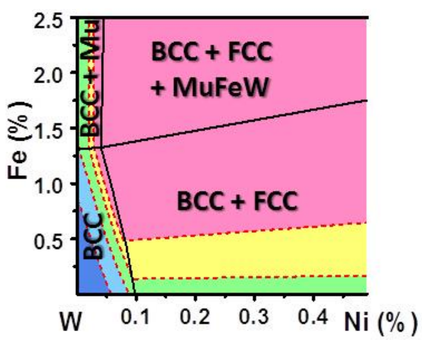

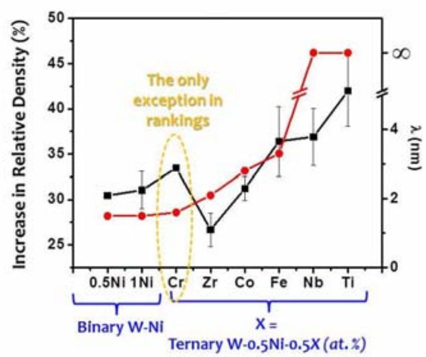

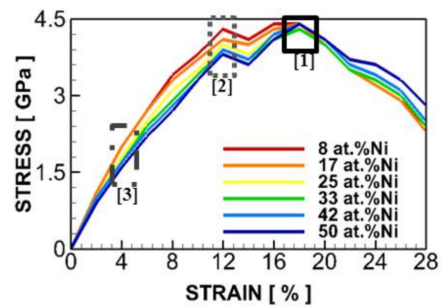

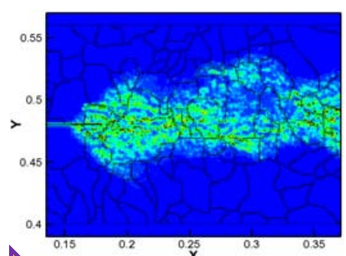

Ternary W-Ni-X (X = Zr, Co, Cr, Fe, Nb, Ti) GB λ-diagrams → Experimental validation → Atomistic & quantum modeling of stress-strain → Continuum facture modeling

Selected Results from Our Year-3 Efforts

Background: Grain Boundary (GB) Segregation
The Classical Models vs. New Perspectives

McLean-Langmuir:

$$\frac{\Gamma}{\Gamma_0 - \Gamma} = \frac{X_C}{1 - X_C} \cdot e^{\frac{-\Delta g_{ads}}{kT}}$$

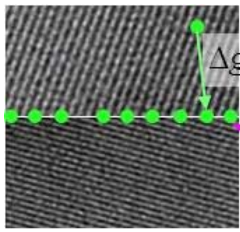

Fowler-Guggenheim:

$$\Delta g_{ads} = \Delta g_{ads}^{(0)} + z_1 \alpha_{\mathrm{Fowler}} \frac{\Gamma}{\Gamma_0}$$

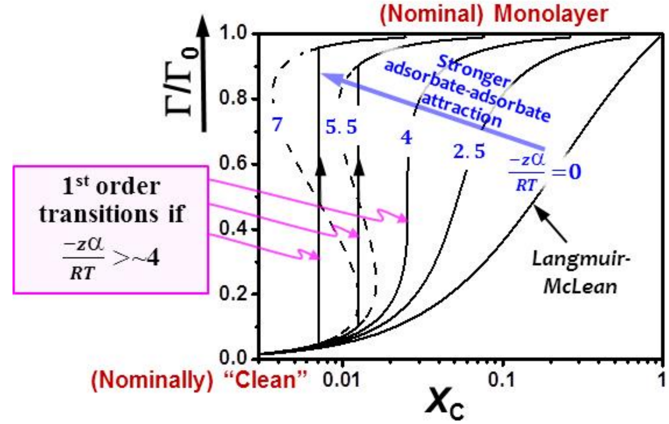

Well-Known Intrinsic GB & Langmuir-McLean type Monolayer/Submonolayer Adsorption

Between Monolayer Adsorption & Complete Wetting

beyond "monolayer"

Discrete Thickness

Continuous (Nanoscale) Thickness

Bilayer **Trilayer**

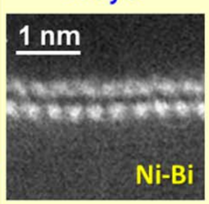

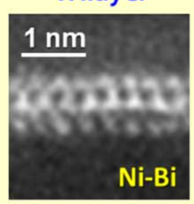

Luo, Cheng, Asl, Kiely, & Harmer *Science* 333: 1730 (2011)

Equilibrium IGF ("Moist")

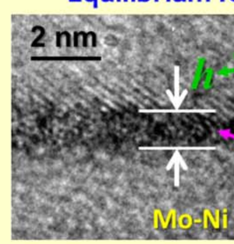

nanoscale "equilibrium" thickness (determined by thermodynamics)

disordered (liquid-like) adsorbates

Shi & Luo, Appl. Phys. Lett. 94: 251908 (2009)

Well-Known Grain Boundary Complete Wetting Film ("arbitrary" thickness)

$h \rightarrow +\infty$

Reprint from Luo,
J. Am. Ceram. Soc. 95:2358 (2012)

Interfacial Width ↑ Adsorption ↑ Structural Disorder ↑

Background: Grain Boundary (GB) Embrittlement
The Classical Models *vs.* New Perspectives

Classical GB Embrittlement Models – Built on Langmuir-McLean Adsorption

Reduction of cohesion due to:
- Electronic effect (weakening the bonds);
- Atomic size (strain) effect; or
- Changing relative γs (the Rice-Wang Model)

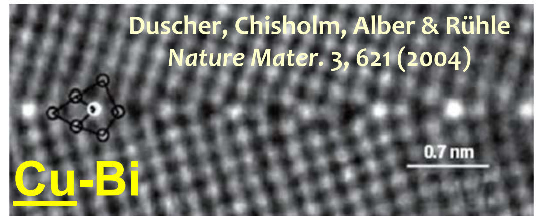

Beyond "Monolayer" ?

New Perspective:
Segregation → GB Transition → Drastic Change in Properties

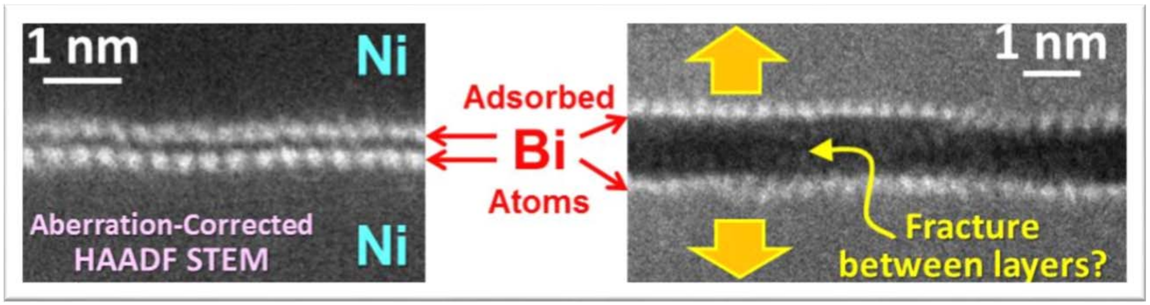

"Complexion" Transition (Bilayer)

Luo, Cheng, Asl, Kiely & Harmer *Science* 333:1730 (2011)

At High Temperatures & Alloying/Impurity Levels…
Segregation → GB "Melting" (Interfacial Disordering) → Embrittlement

Interfacial Disordering
(Liquid-Like GB "Complexion")

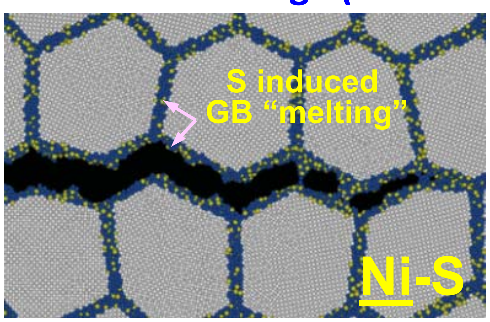

S segregation → GB "melting" if C_S^{GB} > 15%
→ GB Embrittlement

Atomistic Simulation: Chen *et al.*, *PRL* 2010
Auger: Heuer *et al.*, *J. Nuclear Mater.* 2002

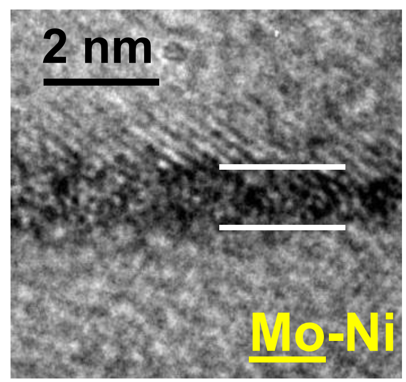

APL 94, 251908 (2009)

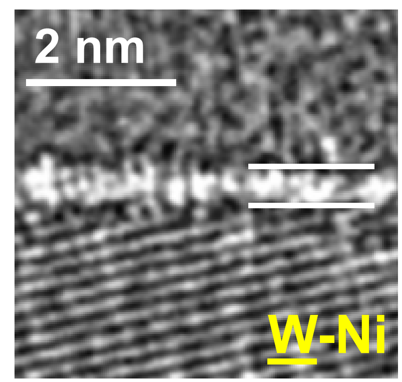

Acta Mater. 55, 3131 (2007)

The Phenomenon

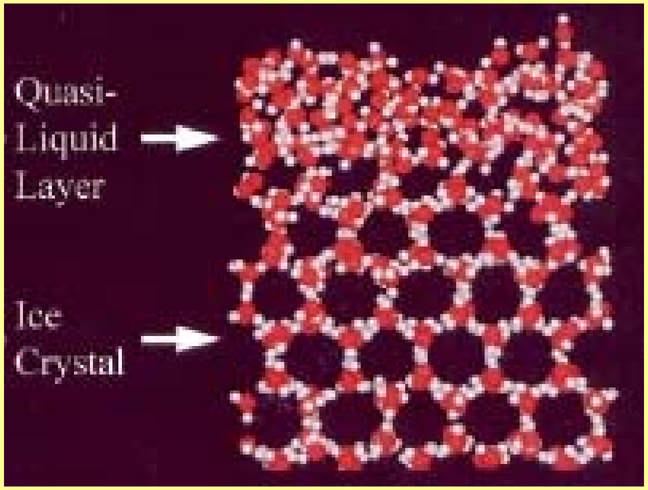

Ice Surface (MD simultaion)
Dash et al, ***Rev. Modern Phys.*** **2006**

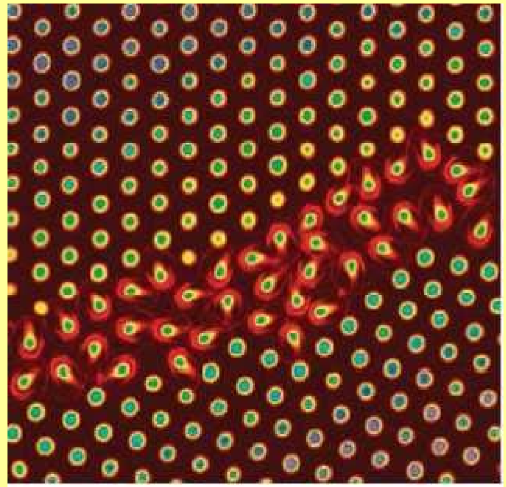

GB premelting in a colloidal crystal
Alsayed et al, ***Science*** **2005**

Unary Systems:

- **Surface Premelting √**
- **GB Premelting ???**

Late 1980's: Balluffi's group suggested no GB premelting up to 0.999T_{melt} in Al!

Thermodynamically stable at
$T < T_{melting}$

Ceramic Systems (Well Known)

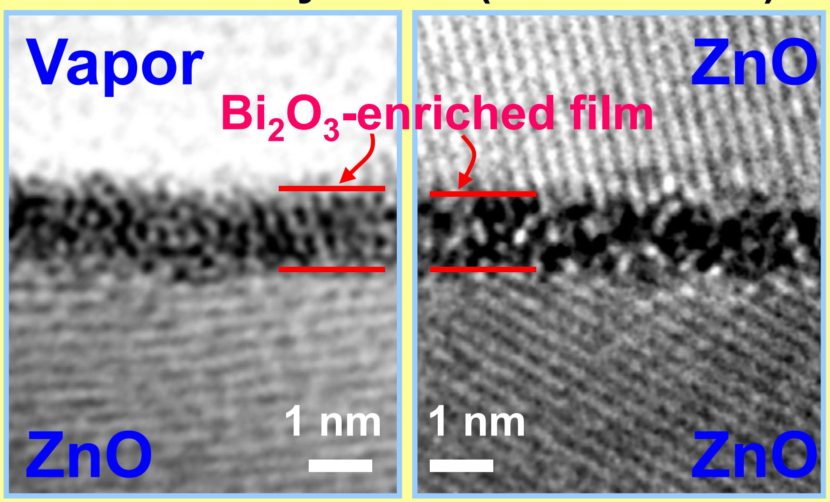

$\Delta T \equiv T_{eutectic} - T = 140°C$ $\Delta T = 40°C$

Luo et al., ***Langmuir*** **2005**   Wang & Chiang, ***JAmCerS*** **1998**

Ni-doped W

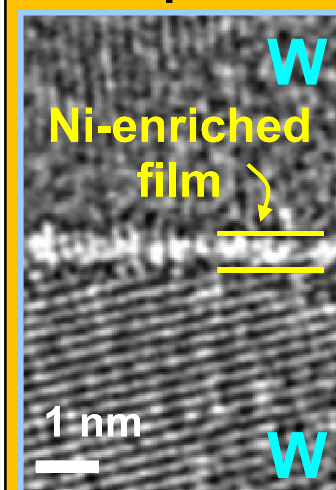

$\Delta T = 95°C$

Luo et al, ***APL*** **2005**

Multicomponent?

- **Enhanced by segregation**

→ **Sintering √ (Prior work)**
→ **Embrittlement √ (This study)**
→ **Coble creep? (Next UCR project)**

Can be stabilized at
$T < T_{solidus}$

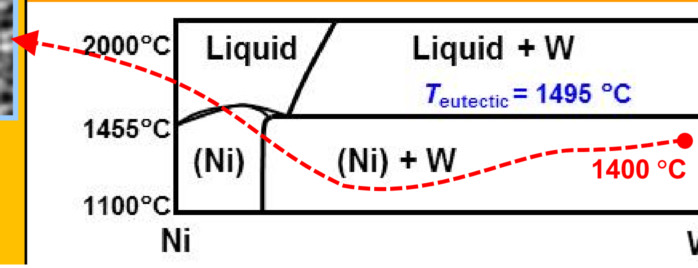

Thermodynamic Principle and Model

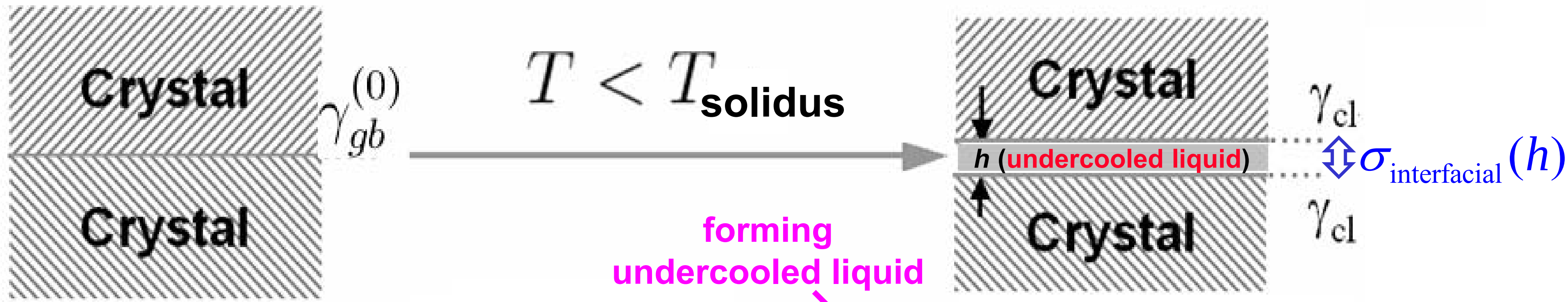

forming undercooled liquid

A subsolidus quasi-liquid film is **thermodynamically stable** if:

$$\Delta G_{\text{amorph}} \cdot h < -\Delta\gamma \equiv \gamma_{gb}^{(0)} - 2\gamma_{cl}$$

Define & quantify:

$$\lambda \equiv \frac{-\Delta\gamma}{\Delta G_{amorph}}$$

Statistical Thermodynamic Model

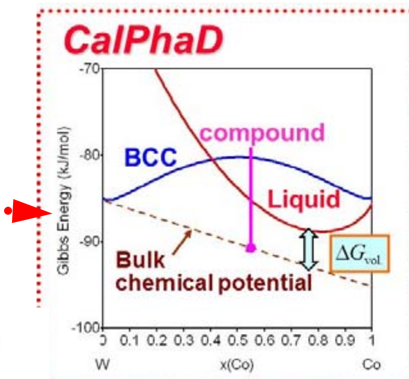

λ represents the thermodynamic tendency to stabilize a quasi-liquid film

λ scales the film thickness

Continuum approx. for metals:

$$h_{EQ} \approx \xi \cdot \ln(\lambda / \xi)$$

Coherent length

A Prior Successful Example of Predictive Modeling: Extending Bulk CalPhaD Methods to GBs

Computed Lines of Constant λ: GB λ-Diagrams

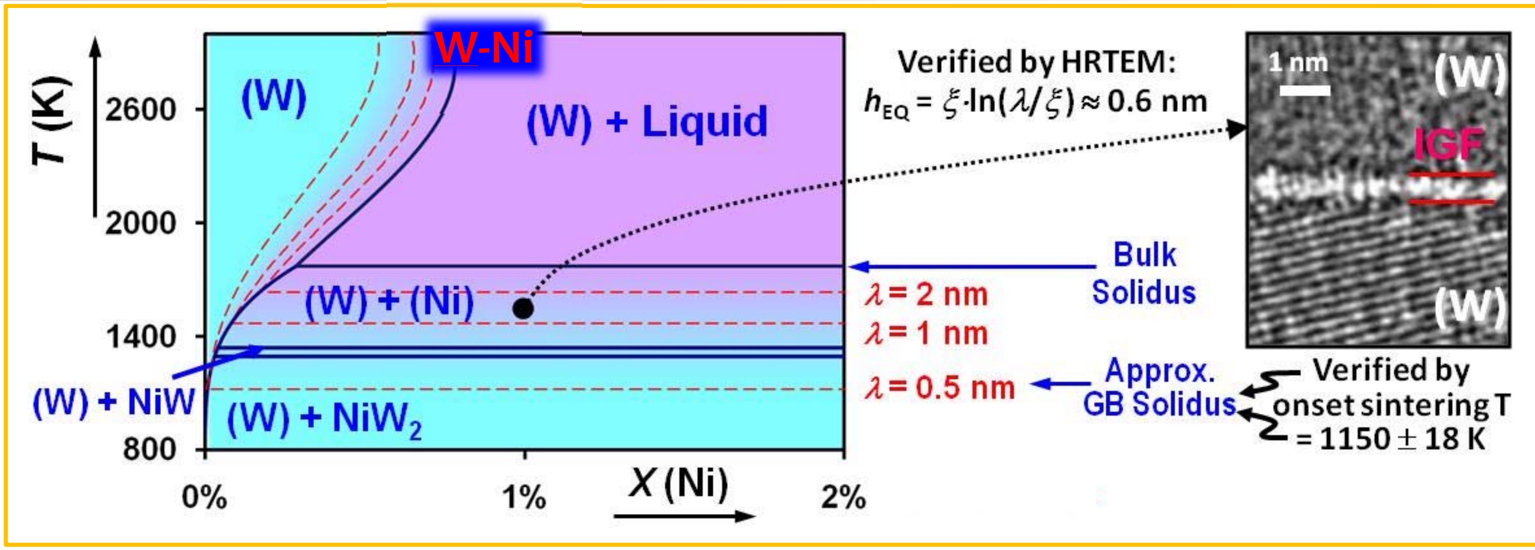

Experimental Validation:

- HRTEM
- Auger
- Onset T_{sinter} for W-X
- $D_{GB}(T, X)$

Computed GB λ-diagram

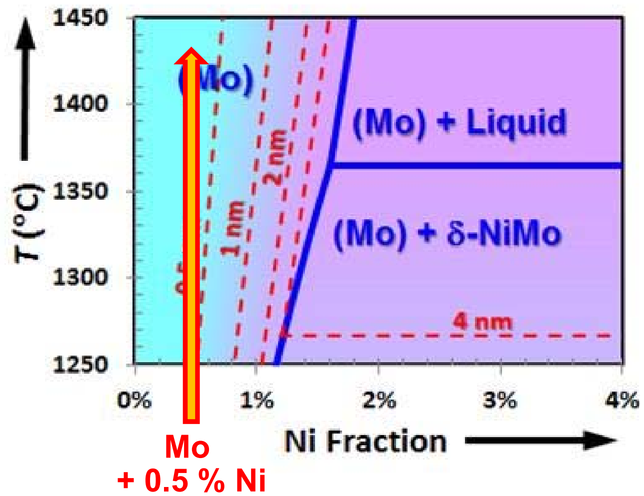

Example of Predictability:

A counterintuitive prediction of D_{GB} ↓ as T ↑ was verified!

Shi & Luo PRL 2010

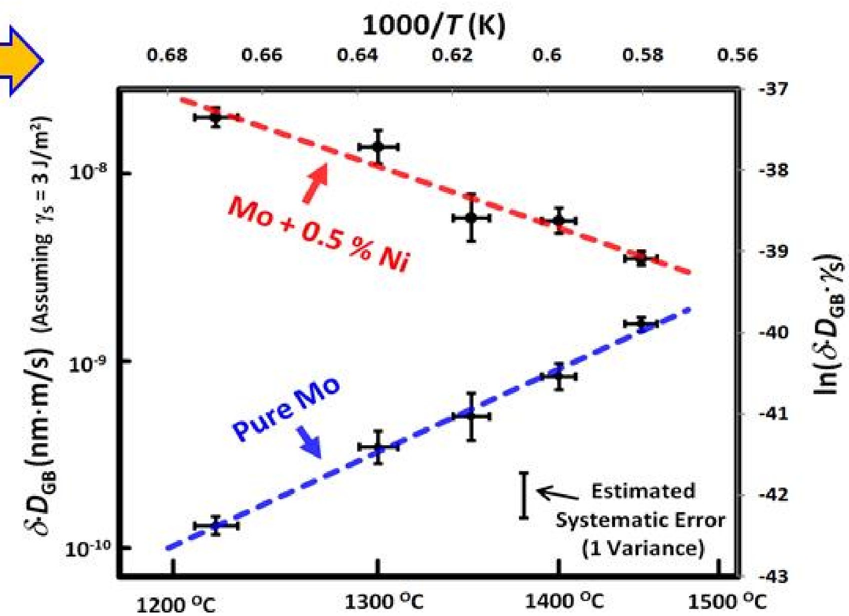

One Major 3rd-Year Task of This UCR Project (as proposed)

Computing Ternary GB λ-Diagrams for W-Ni-X (X = Zr, Co, Cr, Fe, Nb, Ti)

$$\lambda \equiv \mathrm{Max}\left\{\frac{\gamma_{GB} - 2\gamma_{cl}}{\Delta G_{amorph}}\right\}$$

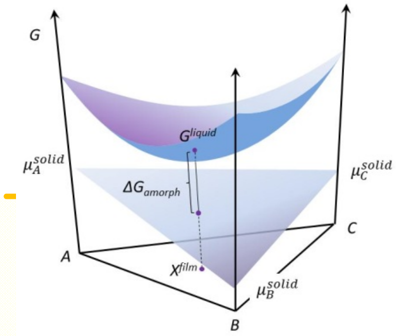

Ternary CalPhaD

$$\Delta G_{amorph}(\mathbf{X}^{film}) = G^{liquid}(\mathbf{X}^{film}) - \sum_i \mu_i^{solid} X_i^{film}$$

Redlich-Kister Expansion

$$G^f(T, X_A, X_B) = X_A G_A^0 + X_B G_B^0 + X_C G_C^0 + RT(X_A \ln X_A + X_B \ln X_B + X_C \ln X_C) + X_A X_B \sum_{j=0}^{n_{AB}} \Omega_j^{AB}(X_A - X_B)^j$$
$$+ X_B X_C \sum_{j=0}^{n_{BC}} \Omega_j^{BC}(X_B - X_C)^j + X_C X_A \sum_{j=0}^{n_{CA}} \Omega_j^{CA}(X_C - X_A)^j + X_A X_B X_C G^{ABC}$$

Statistical Thermodynamic Model (using CalPhaD data)

$$\gamma_{GB} = \frac{H_A^{vapor}}{3C_0 V_A^{2/3}}$$

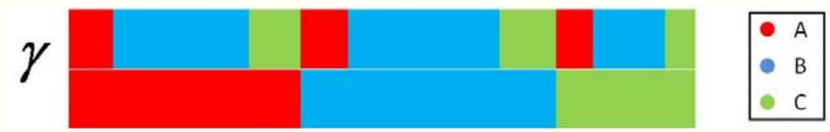

$$\gamma_{cl}(\mathbf{X}^{film}) = \frac{H_A^{fuse}}{C_0 V_A^{\frac{2}{3}}} + \sum_{i \neq A} X_i^{film} \frac{\omega_{i-j}^{liquid}}{C_0 V_A^{\frac{2}{3}}} + \frac{1.9RT}{C_0 V_{Average}^{\frac{2}{3}}} - \sum_{j \neq i} \sum_{i \neq A} \frac{X_i^{film} X_j^{film} \omega_{i-j}^{liquid}}{2C_0 V_A^{2/3}}$$

Practical Importance:

- **Engineering alloys often have many components or impurities**
- **Co-alloying to control GB behaviors?**

Construct A Ternary GB λ-Diagram
(An Example: W-Ni-Fe, 1300 °C)

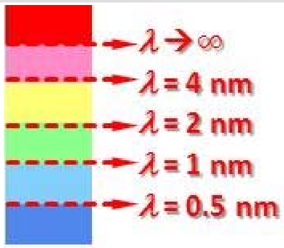

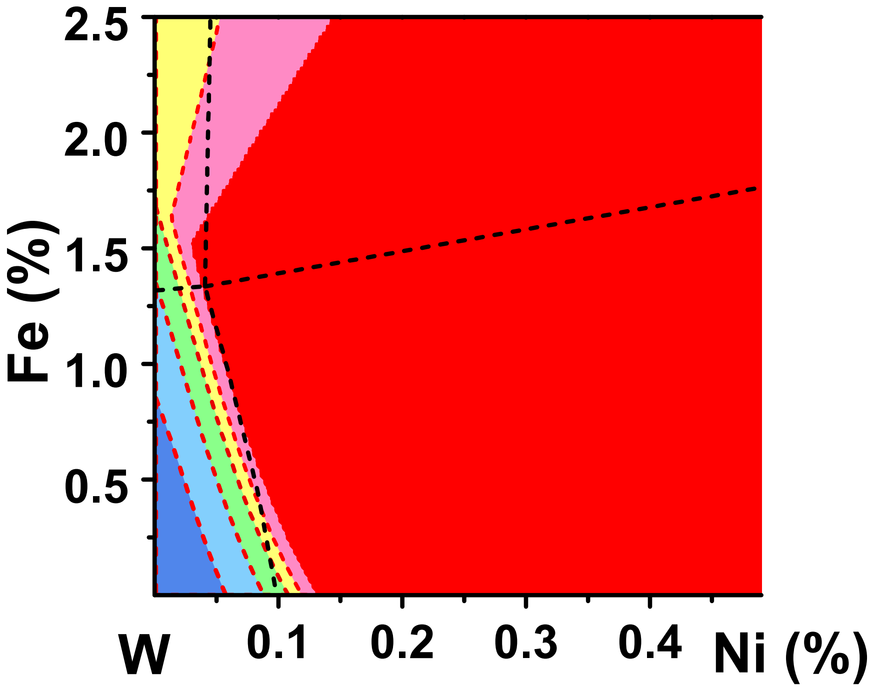

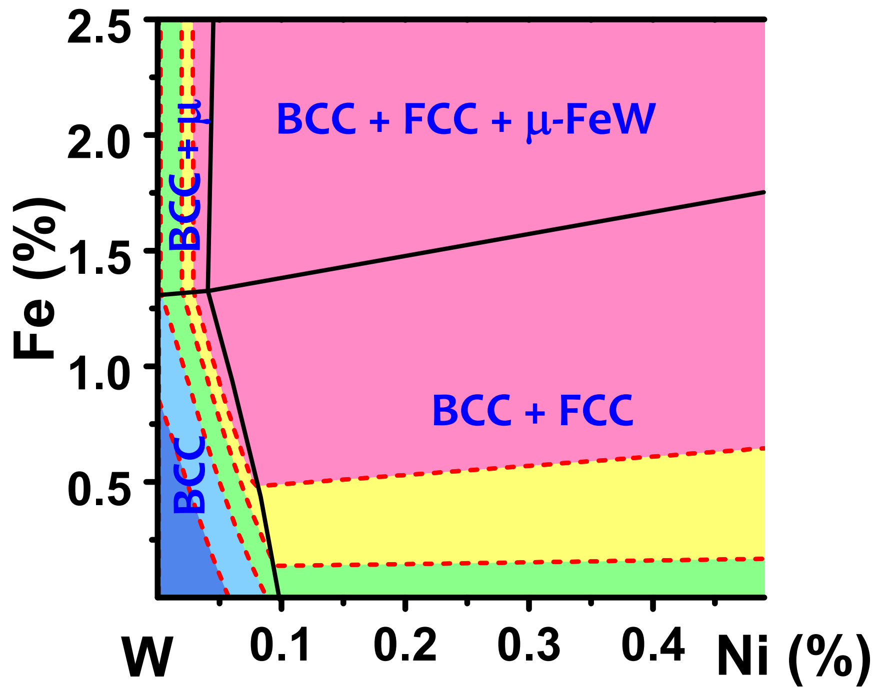

Considering ONLY the W-based BCC phase (& liquid phase)

Considering All Phases @ Bulk Equilibria

Computed W-Ni-X (X = Cr, Zr, Co, Fe, Nb, Ti) Ternary GB λ-Diagram

(Considering Only BCC and Liquid Phases)

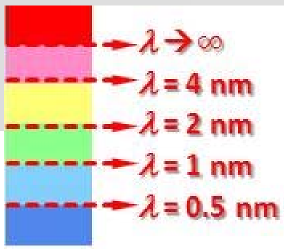

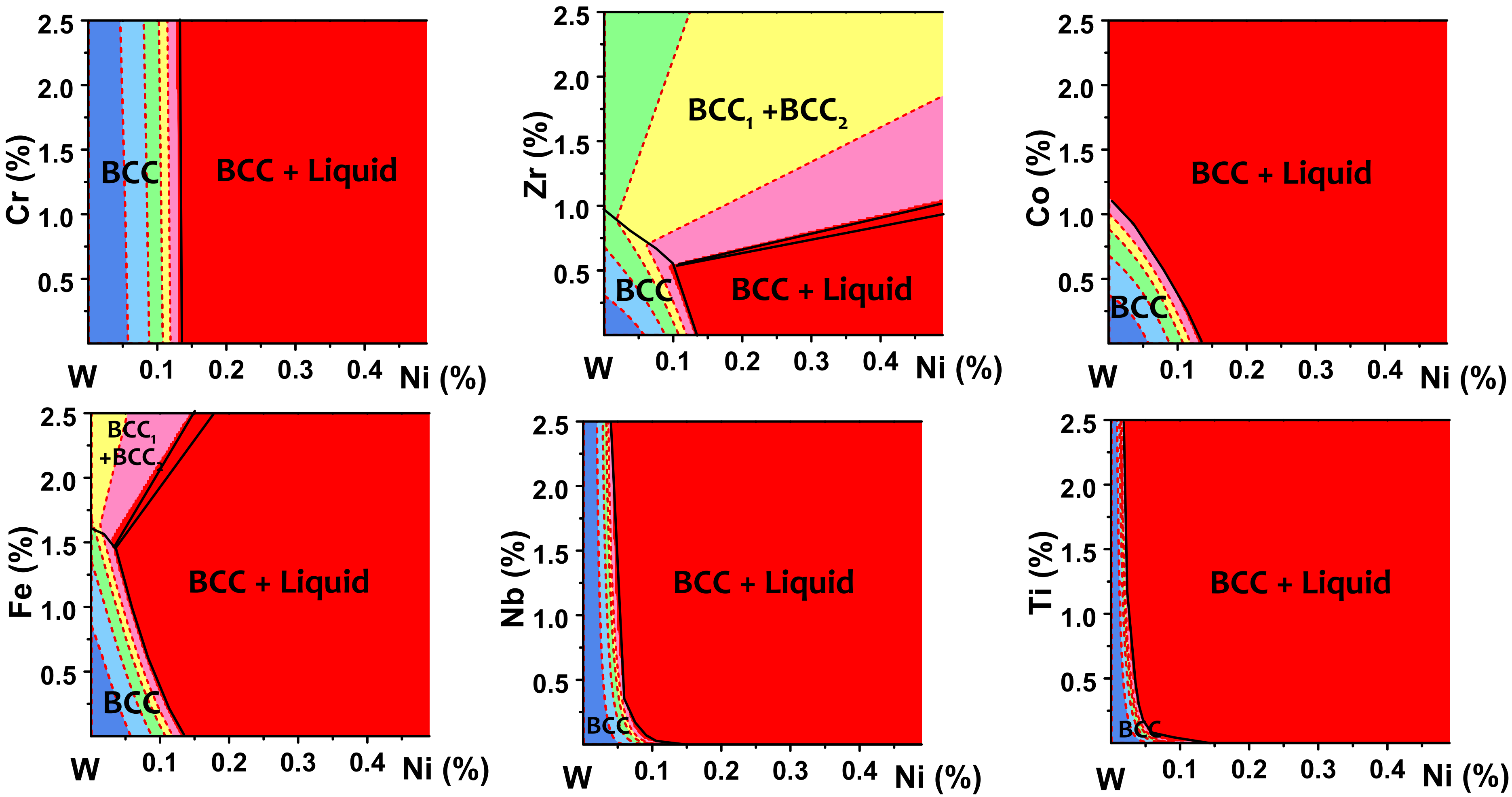

T = 1300 °

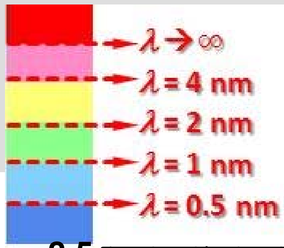

Computed W-Ni-X (X = Cr, Zr, Co Fe, Nb, Ti) Ternary GB λ-Diagram

(Considering All Stable Bulk Phases)

T = 1300 °C

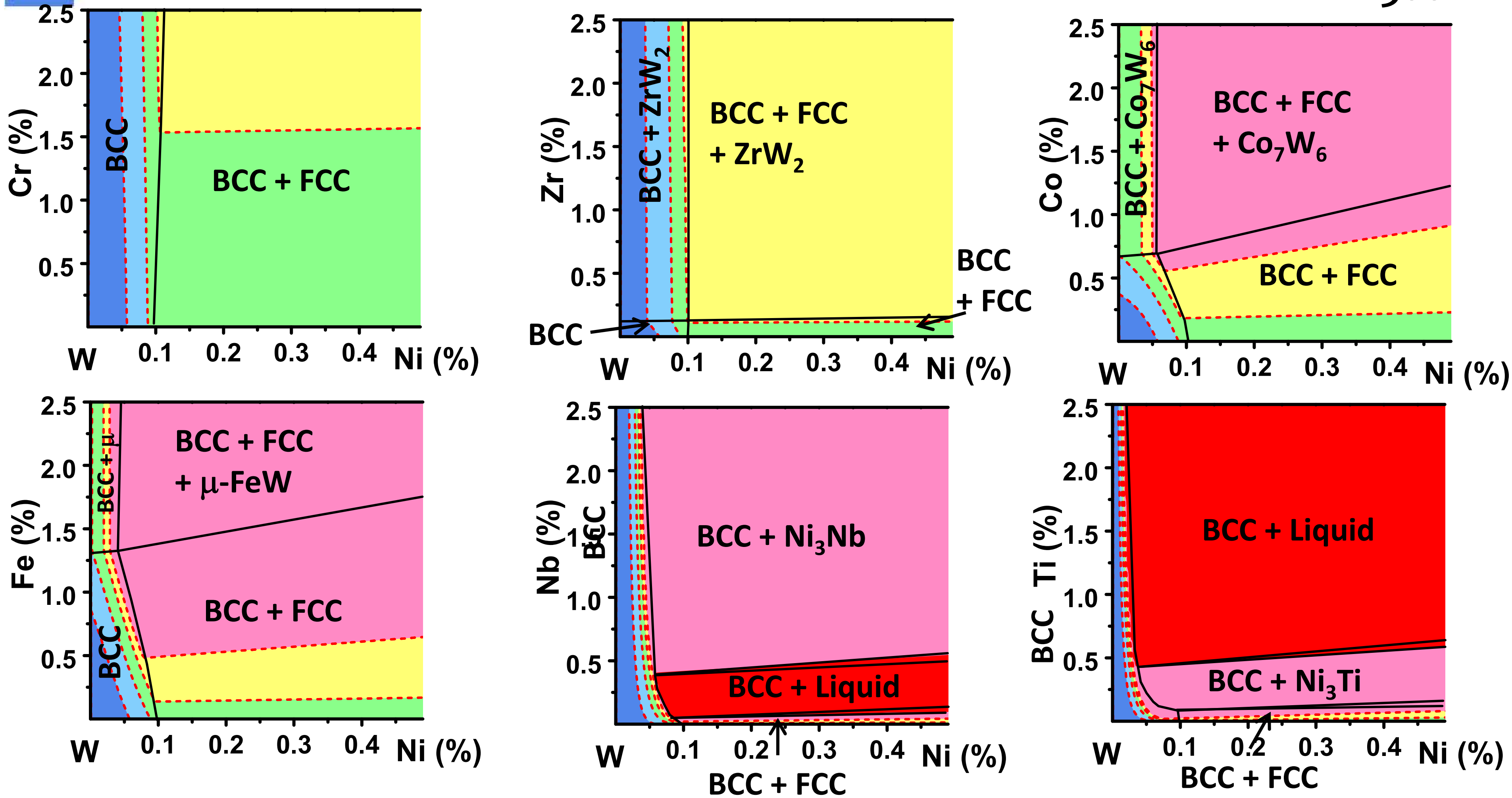

One Prediction: The co-alloying effect on promoting GB disordering of W-Ni-X (represented by the increase in λ) roughly follows the order: Cr < Zr < Co < Fe < Nb <Ti

Experimental Model Validation: Co-doping Effects in Ternary Alloys

For W-Ni-*X* (*X* = Zr, Co, Cr, Fe, Nb, Ti)

A custom-made furnace

- To remove ramping effects

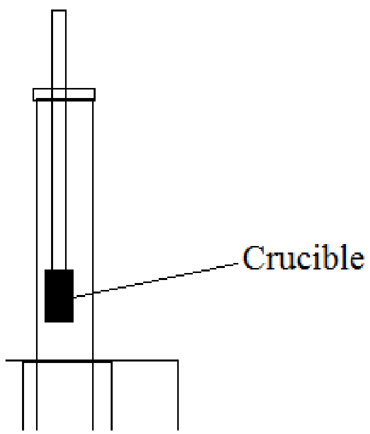

Our Approach:

Density rate → The effect of co-alloying on promoting GB disordering (represented by the increase in computed λ)

Limitation: Chemical effect on GB diffusion not represented

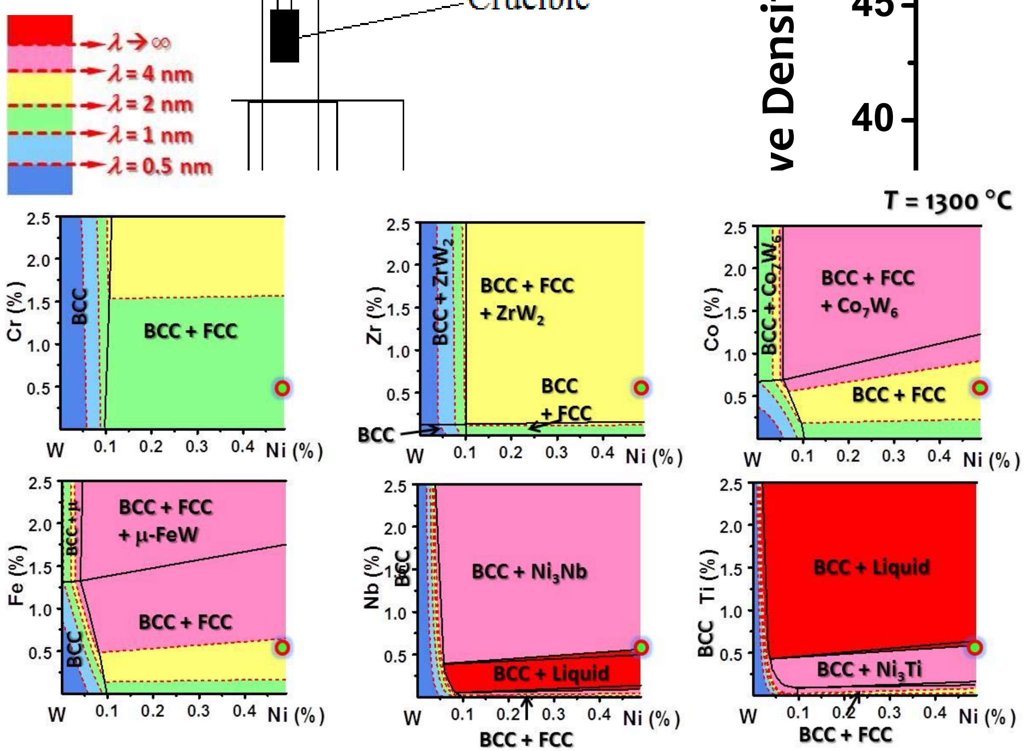

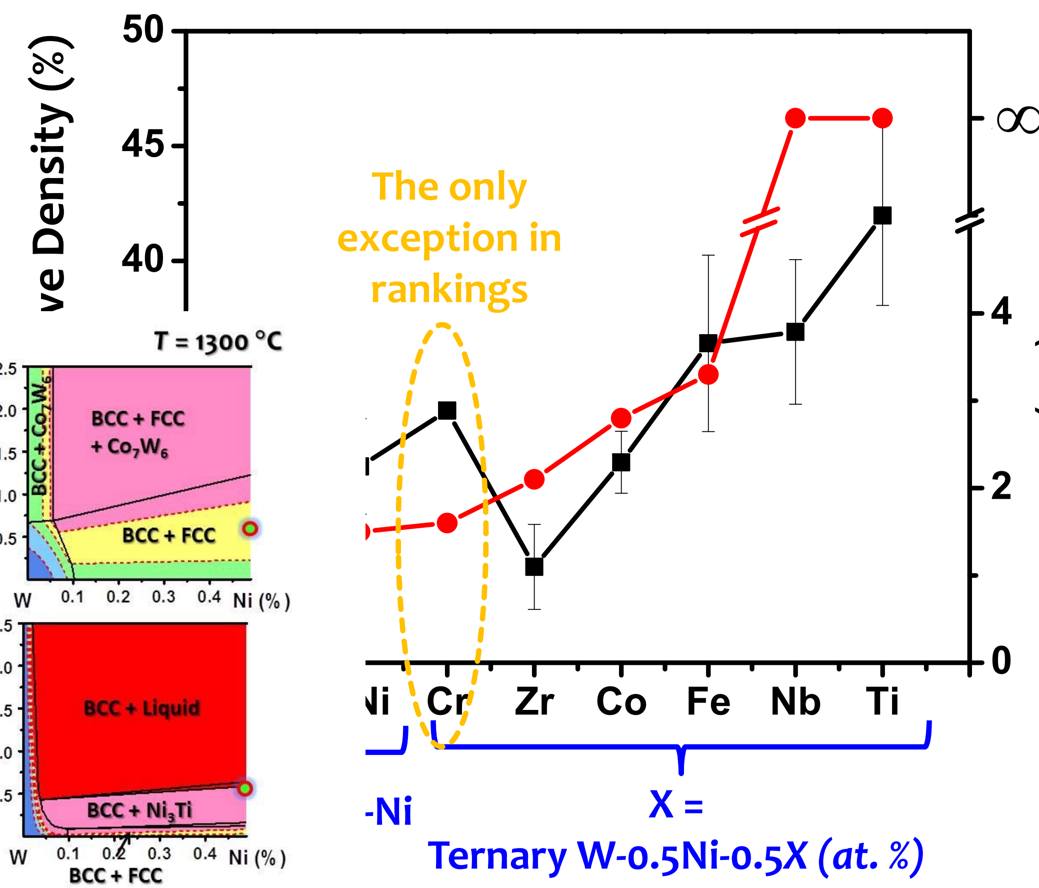

Estimate Interfacial Width (h_{EQ}) from the Computed λ-Diagram?

The Excess Free Energy:

Interfacial (disjoining) Potential

$$G^x - \gamma_{gb}^{(0)} = \Delta G_{amorph}\cdot h + \Delta\gamma + \sigma_{interfacial}(h) = \Delta G_{amorph}\cdot h + \Delta\gamma\cdot f(h)$$

Interfacial coefficient

$$\begin{cases} f(0)\equiv 0 \\ f(\infty)\equiv 1 \end{cases}$$

GB λ-Diagram → **Estimating h_{EQ} (& γ_{GB})**

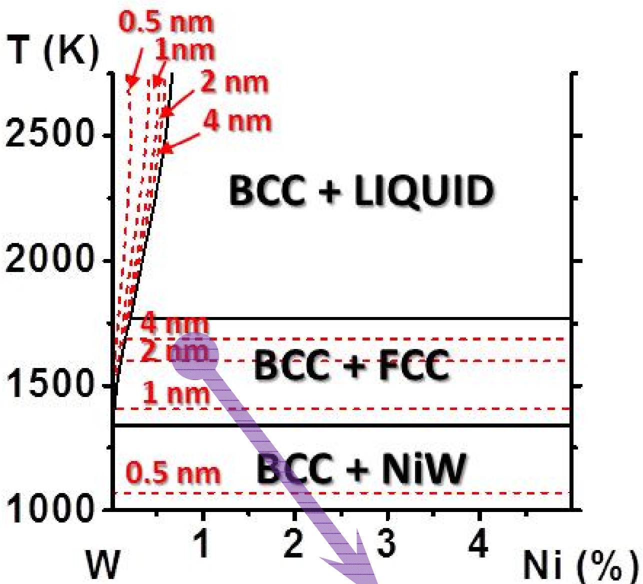

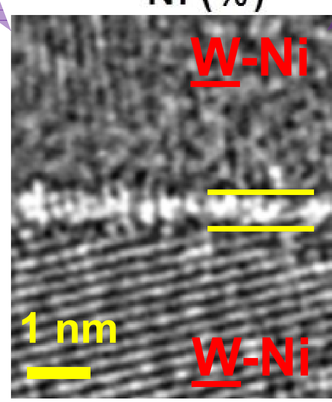

Ni-Saturated W (1400 °C)

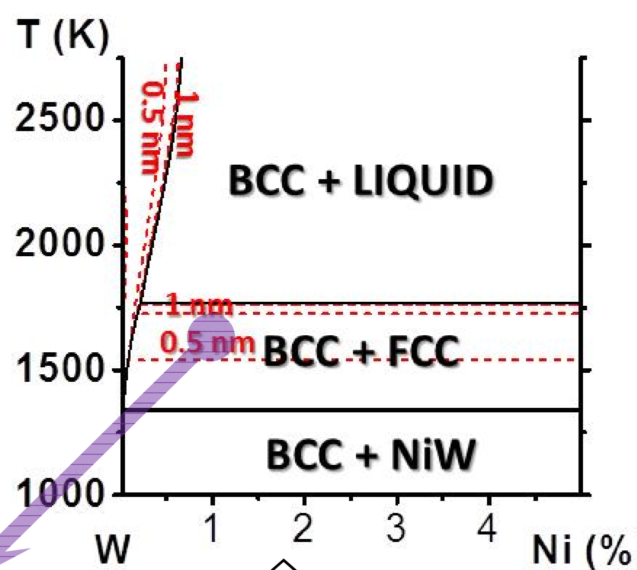

$$\lambda = 2.1\ \text{nm} \Leftrightarrow h_{EQ} = 0.6\ \text{nm}$$

$$\Rightarrow \xi \approx 0.318\ \text{nm}$$

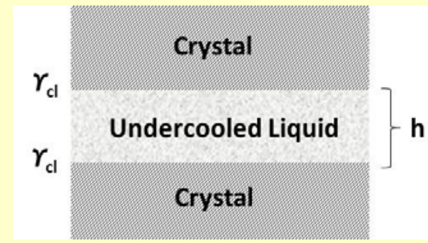

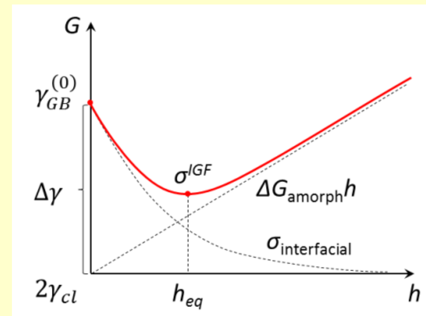

Continuum approx. for metals:

$$f(h) \approx 1 - e^{-h/\xi}$$

Coherent length

$$h_{EQ} \approx \xi \cdot \ln(\lambda/\xi)$$

High-*T* (Liquid-Like) vs. Classic (Solid-Like) GB Segregation

(To Establish a Unified Thermodynamic Framework?)

Premelting-Like Segregation
Interfacial Disordering

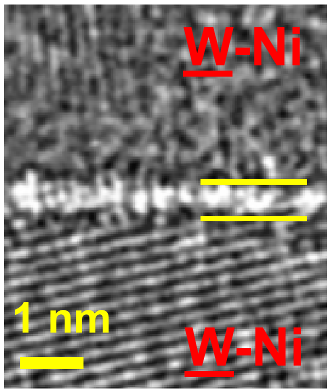

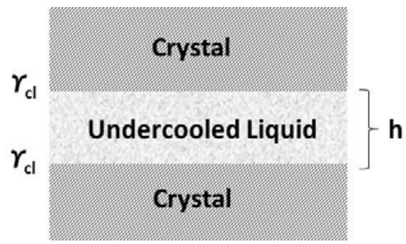

Multilayer Segregation on the Lattice
Wynblatt-Chatain [*JMS* 2005; 2006, *MMA* 2006]

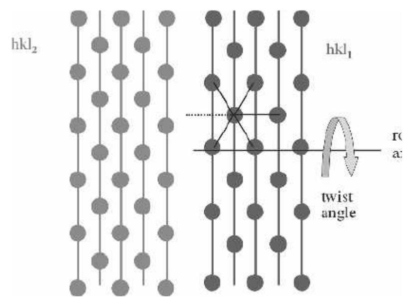

$$\ln\frac{x^i}{1-x^i} = \ln\frac{x}{1-x} - \frac{\Delta H^i_{seg}}{RT}$$

Segregation Enthalpy

GB Core:

$$\Delta H^i_{seg} = 2\omega\Big[zx - z^i x^i - \sum_{j=1}^{J_{max}} z^j x^{i+j} - \sum_{j=1}^{i-1} z^j x^{i-j} - P\sum_{j=1}^{J_{max}} z^j x^j - \frac{1}{2}(1-P)\sum_{j=1}^{J_{max}} z^j\Big] - \frac{1}{2}(1-P)(\varepsilon_{BB}-\varepsilon_{AA})\sum_{j=1}^{J_{max}} z^j - \Delta E^i_{el} \quad [36a]$$

Inside:

for $i \le J_{max}$, *i.e.*, planes with less than the bulk coordination, and by

$$\Delta H^i_{seg} = 2\omega\Big[zx - z^i x^i - \sum_{j=1}^{J_{max}} z^j (x^{i+j} + x^{i-j})\Big] - \Delta E^i_{el} \quad [36b]$$

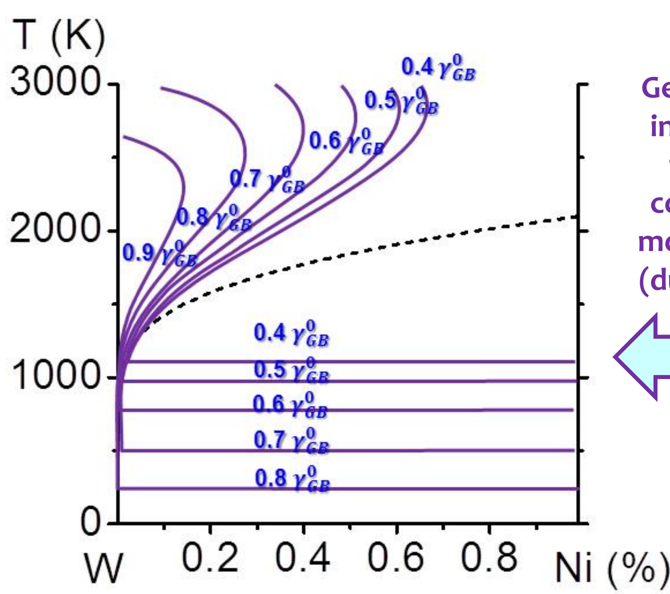

Generally, more reduction in the GB energies (γ_{GB}'s) for forming liquid-like complexions in W-Ni and most other W-based alloys (due to the high $\gamma_{GB}{}^{o}$ of W)

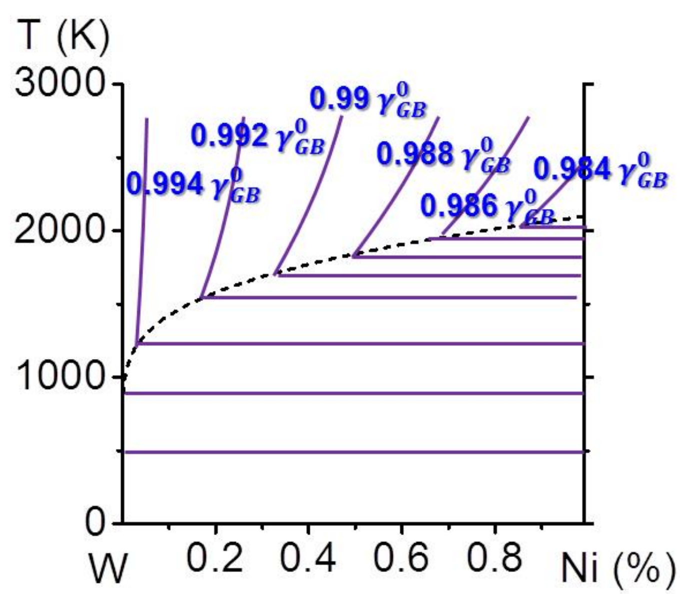

A Useful Component for the "Materials Genome" Project?

Construct "Grain Boundary (GB) Diagrams"

GB λ-Diagrams

(To Predict Useful Trends for GBs to Disorder)

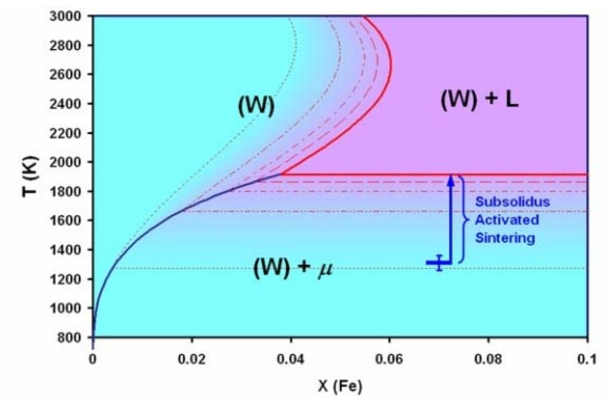

More Rigorous GB Complexion ("Phase") Diagrams ???

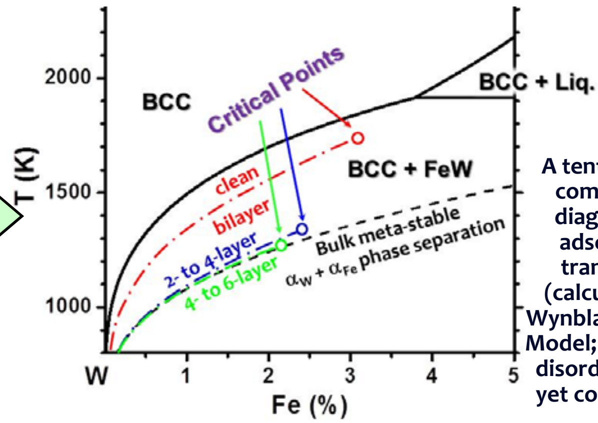

A tentative GB complexion diagram for adsorption transitions (calculated by Wynblatt-Chatain Model; interfacial disordering not yet considered)

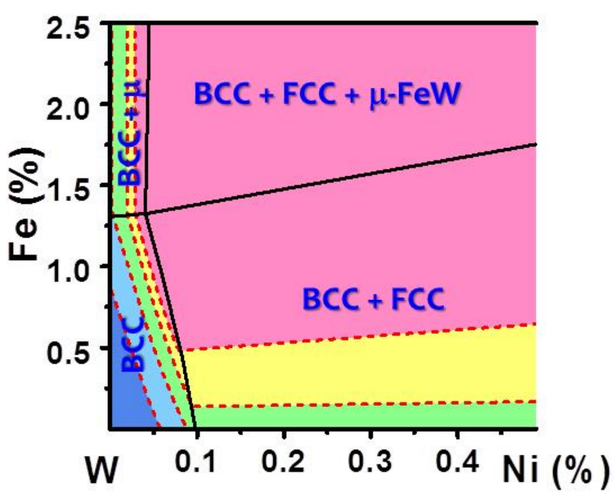

Useful Materials Science Tool for Designing:

- **Fabrication protocols utilizing appropriate GB structures to achieve optimal microstructures**
- **Co-doping strategies and/or heat treatment recipes to tune the GB structures for desired performance**

Applications: To predict useful trends in:

- **GB embrittlement**
- **Sintering**
- **Grain growth & microstructural involution**
- **Coble creep**
- **GB controlled corrosion & oxidation**
- **…**

Following the late Dr. R. M. Cannon's transformative concept

Prior work : Straumal et al., Interf. Sci. 2004; Tang et al., PRL 2006; Dillon et al. Acta Mater. 2007 & more

Summary – Thermodynamics Thrust

We have …

- **(Years 1 & 2) Derived the basic equations;**
- **(Years 1 & 2) Developed and tested the algorithms and MATLAB codes;**
- **(Years 2) Completed numerical experiments;**
- **(Year 3) Computed "GB λ-diagrams" for W-Ni-*X* (*X* = Cr, Zr, Co, Fe, Nb & Ti) systems;**
- **(Year 3) Conducted experimental validation for ternary W alloys;**
- **(Year 3) Compared with classical segregation model in an effort to establish a unified framework; and**
- **Worked closely with the Purdue team to use our thermodynamic models and experimental results to support their multiscale modeling efforts to link GB segregation to mechanical properties.**

PROBLEM DESCRIPTION

- **The primary site of embrittlement of Nickel (Ni) – doped Tungsten (W) is at the grain boundary (GB).**
- **GB is interfacial region between two differently oriented W grains.**
- **Most of the Ni impurities concentrate at the GB region.**
- **GB thickness varies upon the level of saturation. (unsaturated:0.3nm, saturated:0.6nm)**
- **While the mechanical properties (yield stress, ultimate tensile strength, etc) of Ni-doped W varies by the change of Ni amount and the level of saturation, the quantitative relation to predict those mechanical properties are needed.**

PROBLEM DESCRIPTION

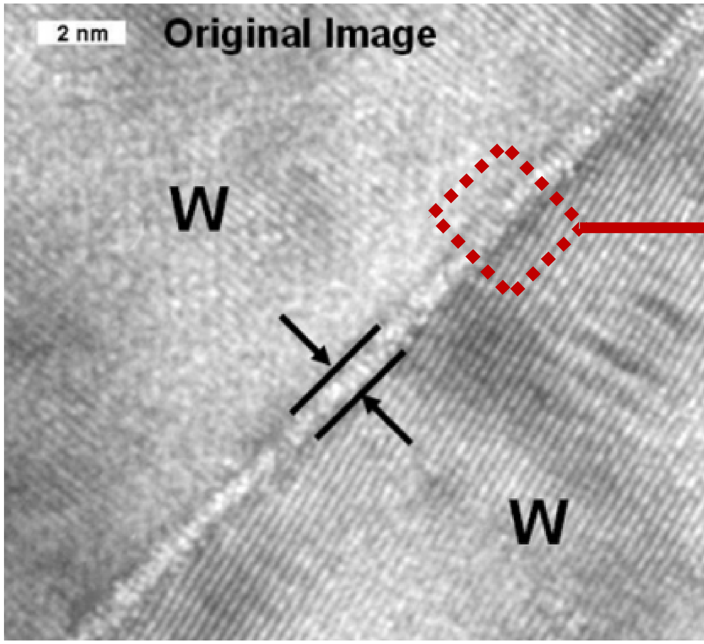

J. Luo and et al, 2005, APL

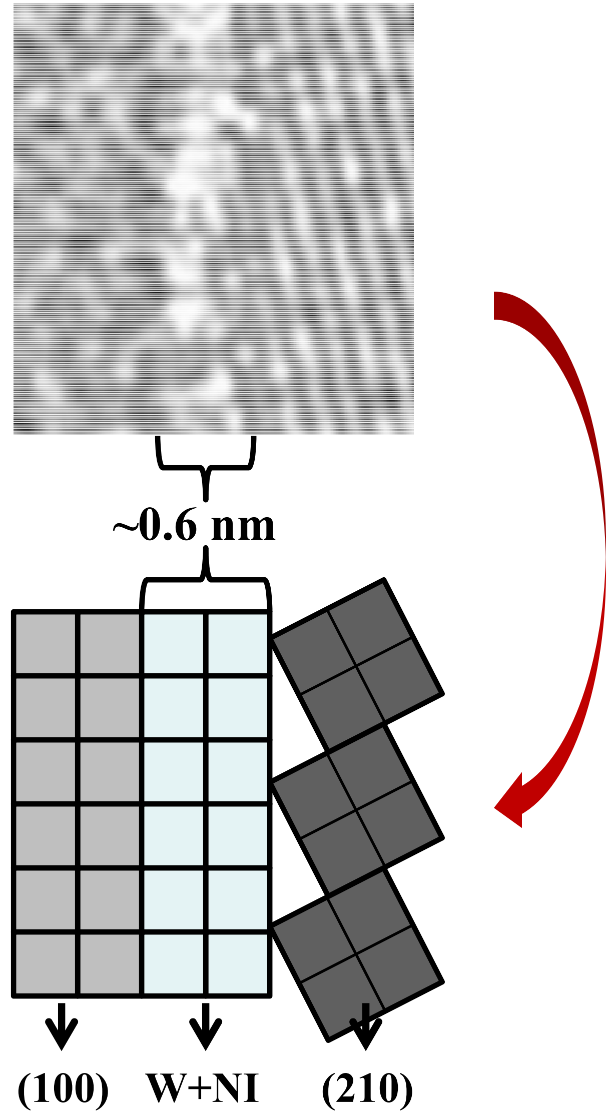

Fully saturated tungsten
→GB thickness = 0.6nm

Consist of (100) and (210) orientation of atom array

Setup

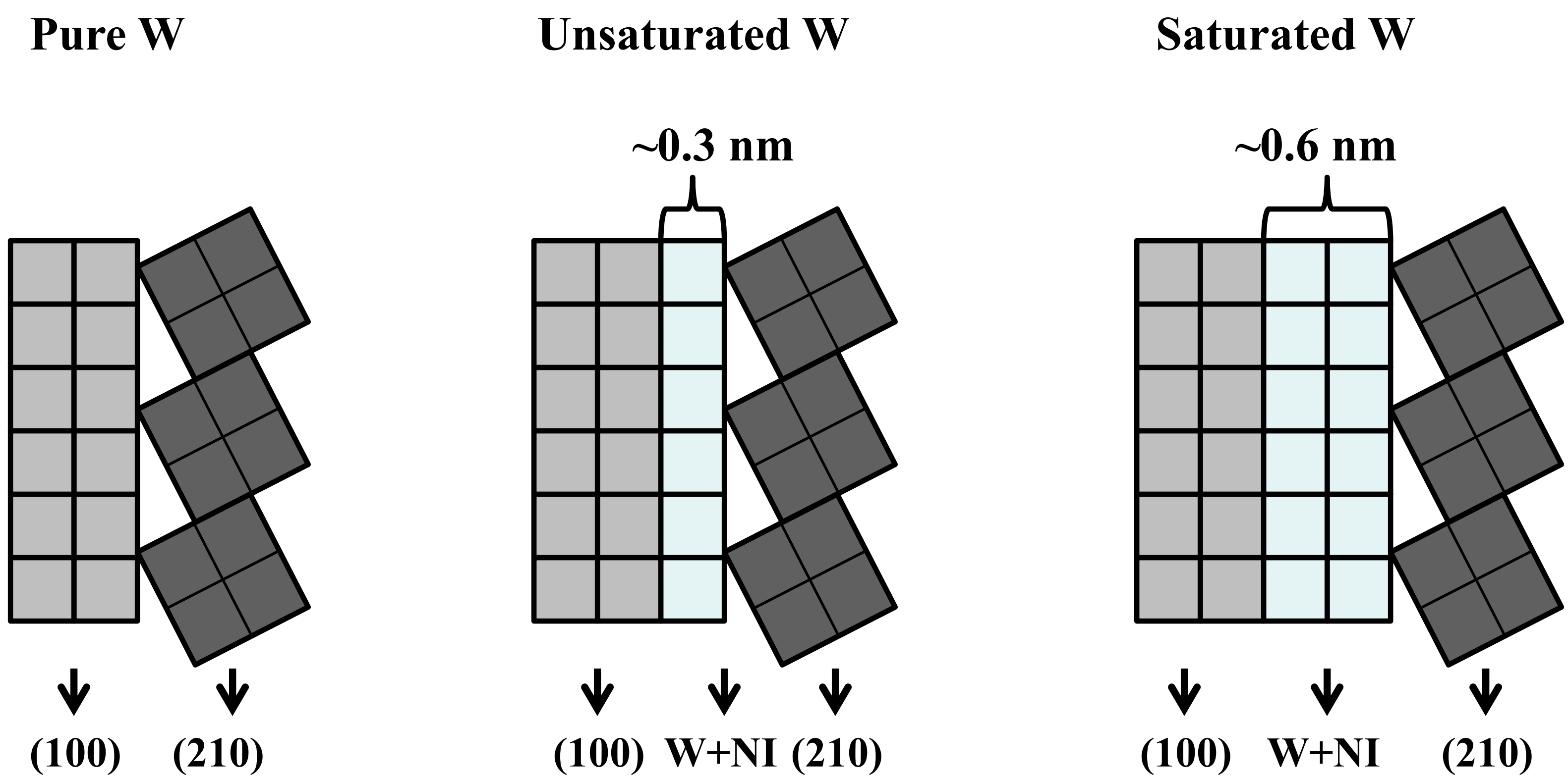

Pure W
Unsaturated W
Saturated W
~0.3 nm
~0.6 nm
(100)
(210)
(100)
W+NI
(210)
(100)
W+NI
(210)

(a) (b) (c)

Setup

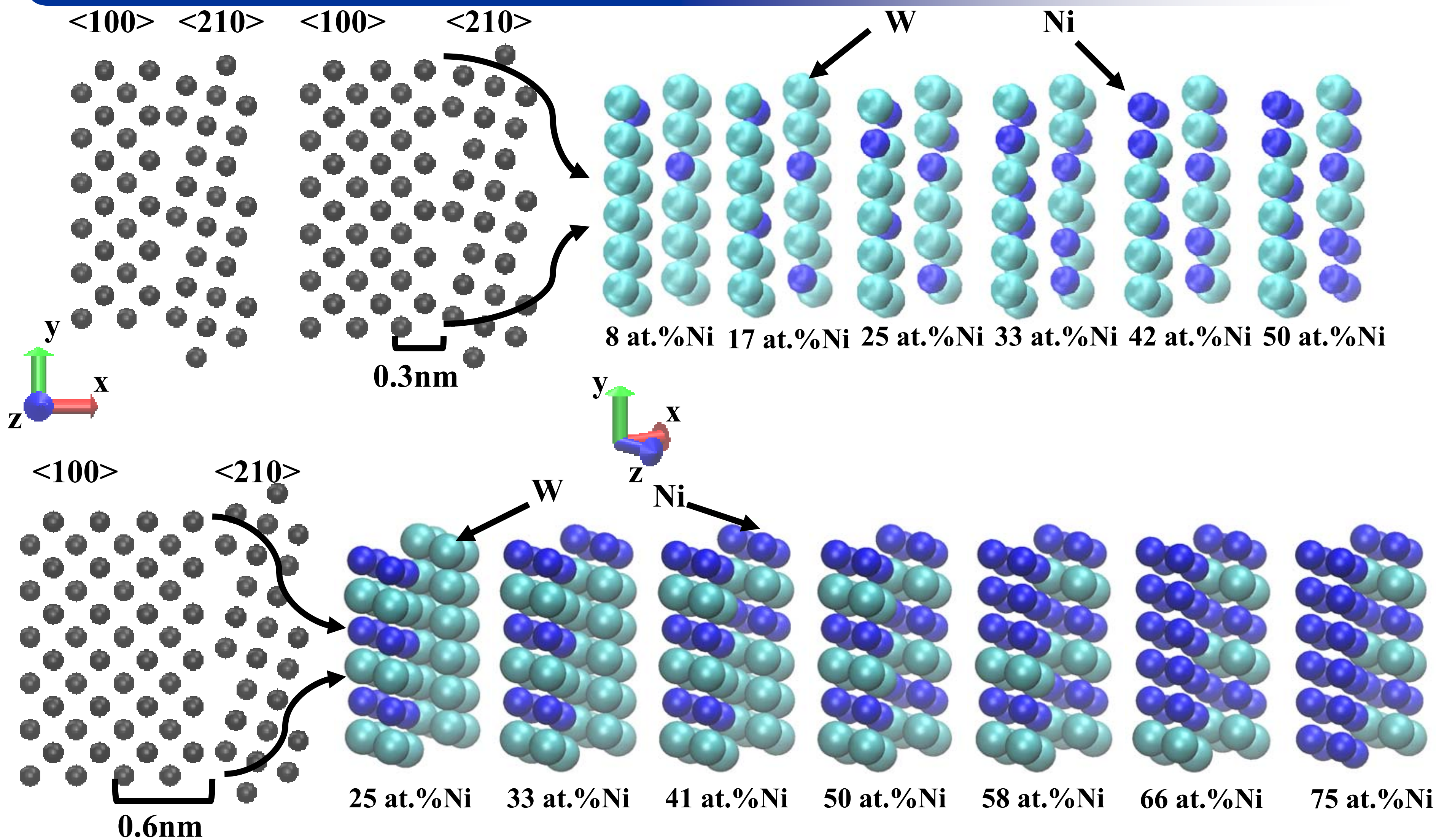

<100>
<210>
<100>
<210>
W
Ni
8 at.%Ni
17 at.%Ni
25 at.%Ni
33 at.%Ni
42 at.%Ni
50 at.%Ni
y
x
z
0.3nm
y
x
z
<100>
<210>
W
Ni
25 at.%Ni
33 at.%Ni
41 at.%Ni
50 at.%Ni
58 at.%Ni
66 at.%Ni
75 at.%Ni
0.6nm

RESULT – (1) PURE W

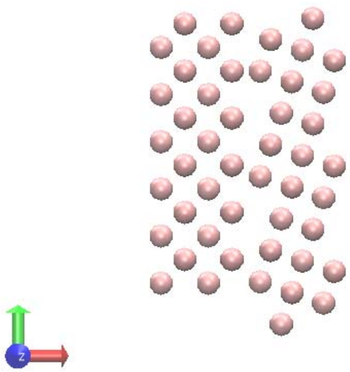

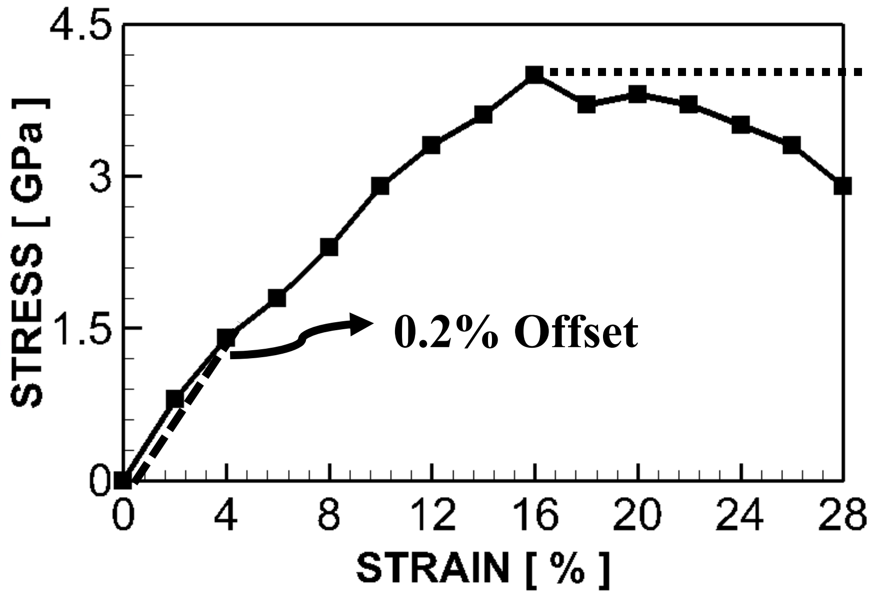

4.0 Gpa **: Ultimate Tensile Strength**

Yield strength : 1.5 GPa at 0.04 strain (approximated by 0.2% offset)

Typical tungsten properties:

Tensile strength : 1.5 ~ 4.2 GPa

Young's modulus : 360 ~ 420 GPa

Q.Wei and et al, 2006, Acta Materialia

RESULT – (2) UNSATURATED (GB thickness = 0.3 nm)

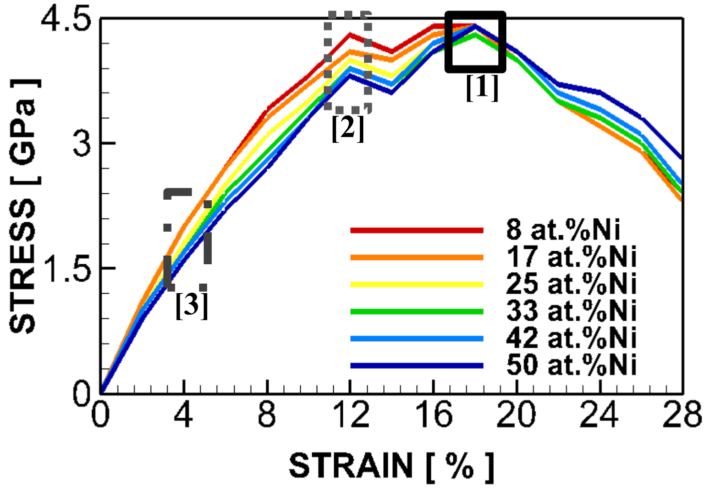

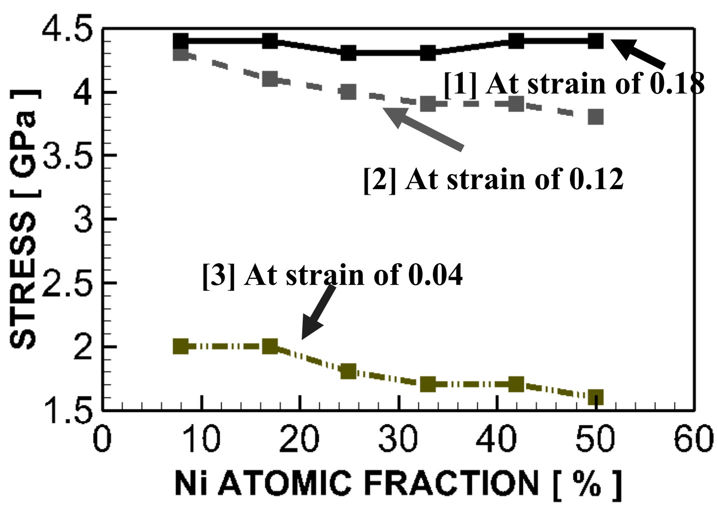

Yield strength: at strain 0.04
The yield strength has dependent on the Ni volume fraction.

First peak: at strain 0.12
The first peak's values has dependent on the Ni volume fraction.

Second peak: at strain 0.18
The second peak's values are not depend on the Ni volume fraction.

Ultimate tensile strength : strain of 0.12~0.18
The maximum tensile strength are not depend on the Ni volume fraction for the unsaturated Ni-doped W.

RESULT – (3) SATURATED (GB thickness = 0.6 nm)

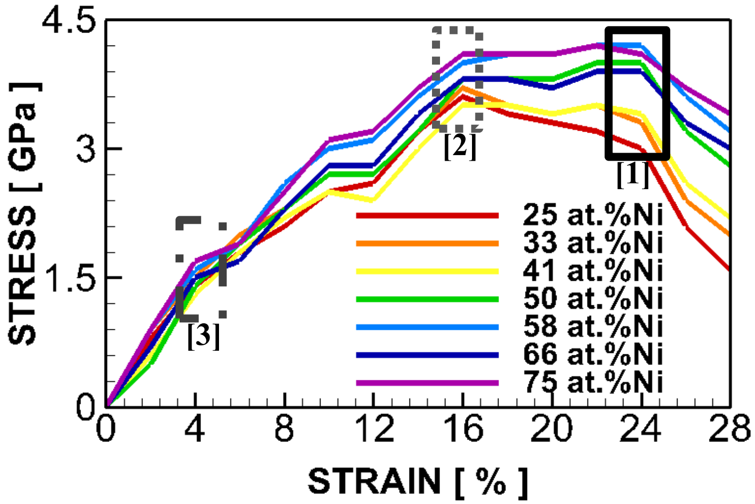

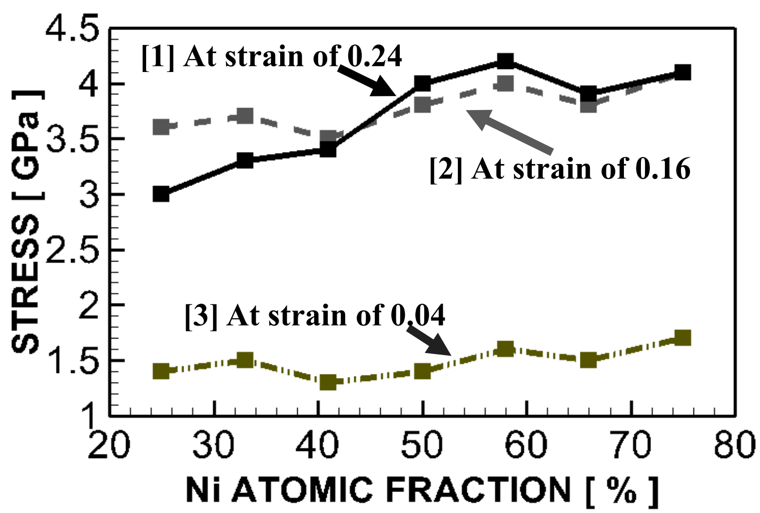

Yield strength: at strain 0.04
The yield strength has dependent on the Ni volume fraction.

First peak: at strain 0.16
The first peak's values has dependent on the Ni volume fraction.

Second peak: at strain 0.24
The second peak's values have the largest dependence on the Ni volume fraction.

Ultimate tensile strength : strain of 0.16~0.24
The maximum tensile strength are depend on the Ni volume fraction for the saturated Ni-doped W.

RESULT – Electron DOS

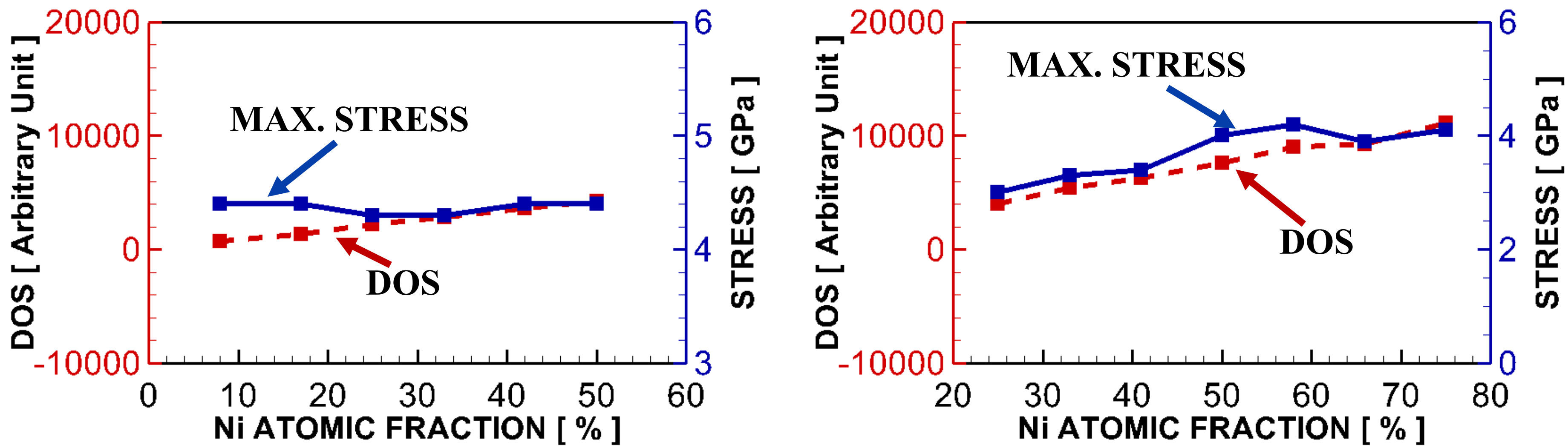

Comparison of the maximum tensile stress with the density of states (sum in the range of -1.3 ~ -1.0 eV) for f-orbital of unsaturated case saturated case

PHONON DISPERSION

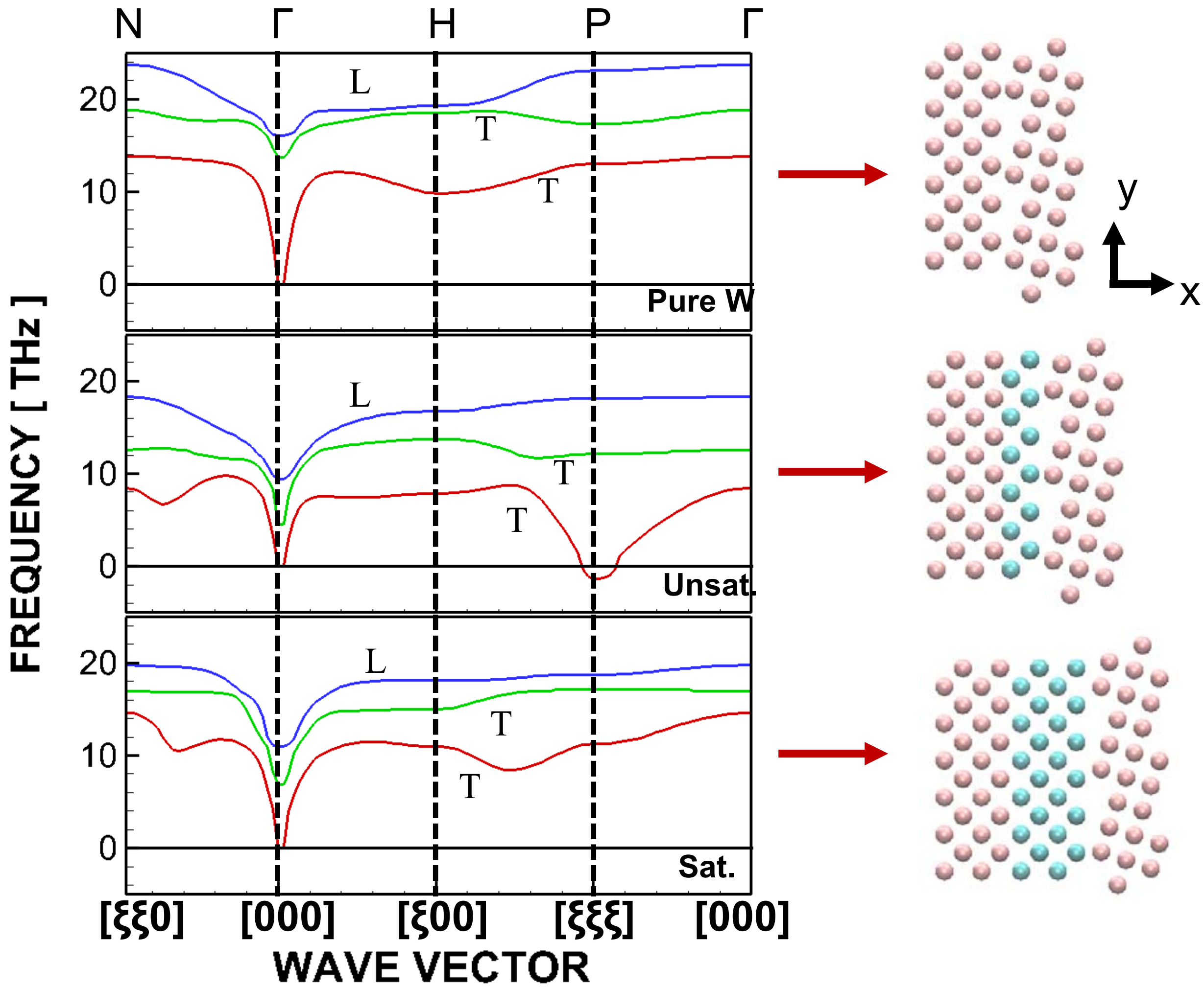

PHONON DISPERSION

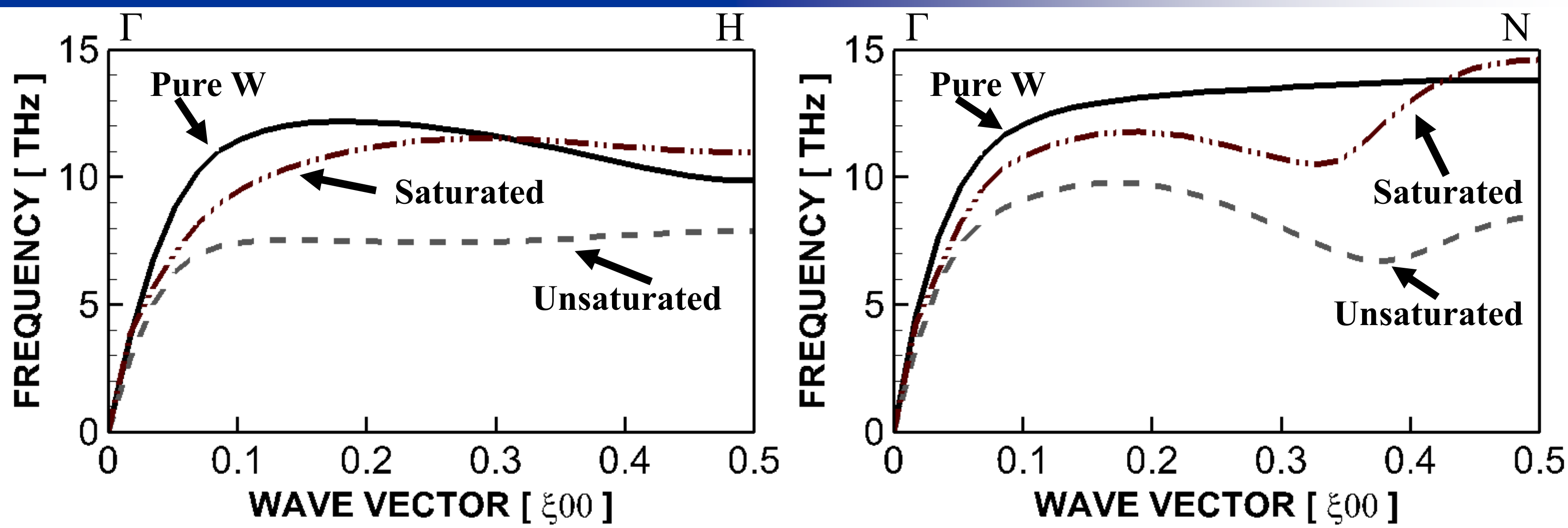

- 1st transverse curve for the direction of [ξ00], and [ξξ0].

- Note that the pure W is idealistic atomic structure based on no GB assumption.

- With existing of GB thickness larger than 0, more saturated form gives higher frequency which is related to the higher bond strength along the horizontal direction.

- Although the atomic structure of pure W provides higher phonon frequency in overall, the stress-strain curve tells us that the substitution of Ni atoms with W plays a role of compensating the low frequency of phonon dispersion curve.

RELATION

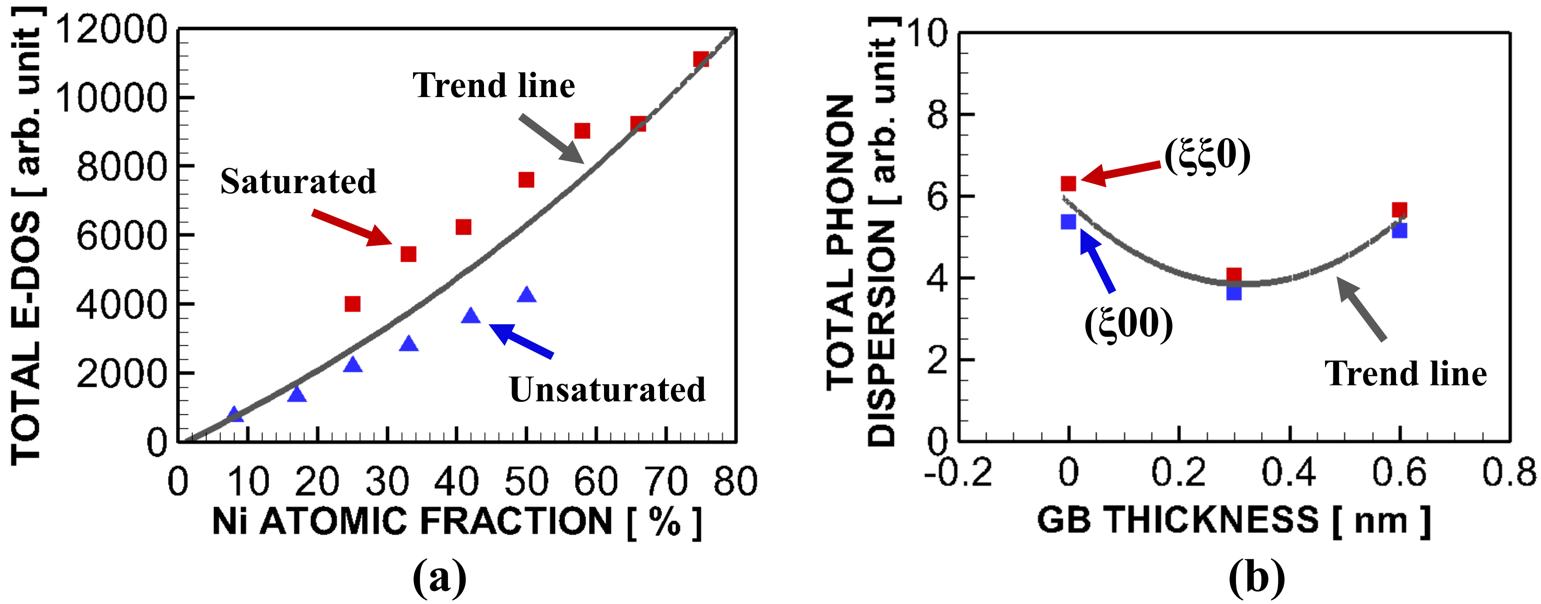

Cubic polynomial regressions for (a) total values of E-DOS (electron density of states) of unsaturated and saturated Ni-added W GB, (b) total values of phonon dispersion in direction of (ξ00) and (ξξ0)

$$\frac{T_{max}}{T_{ideal}} = \frac{CE}{CD}\frac{1}{\Phi} f(t,n)g(w)$$

RELATION

$$T_{max} = T_{ideal} \frac{CE}{CD} \frac{1}{\Phi} \left(e^{n/10} - \frac{t}{t_{melt}} + 6.5 \right) \left(1 - 10^9 w + (10^9 w)^2 \right)$$

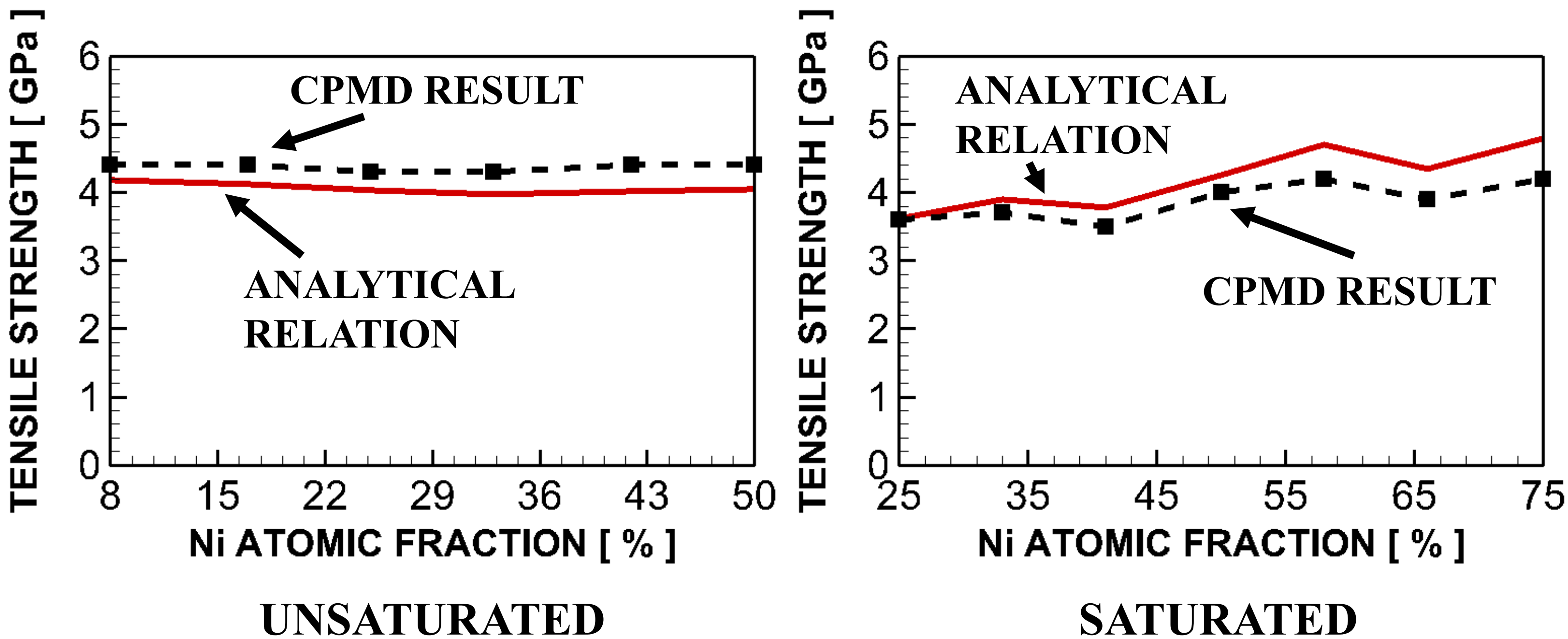

A comparisons of the GB strength as a function of Ni atomic fraction using the derived analytical expression and the CPMD results in the case of 0.3 nm thickness GB, and 0.6 nm thickness GB

OBTAINING MICROSTRUCTURES

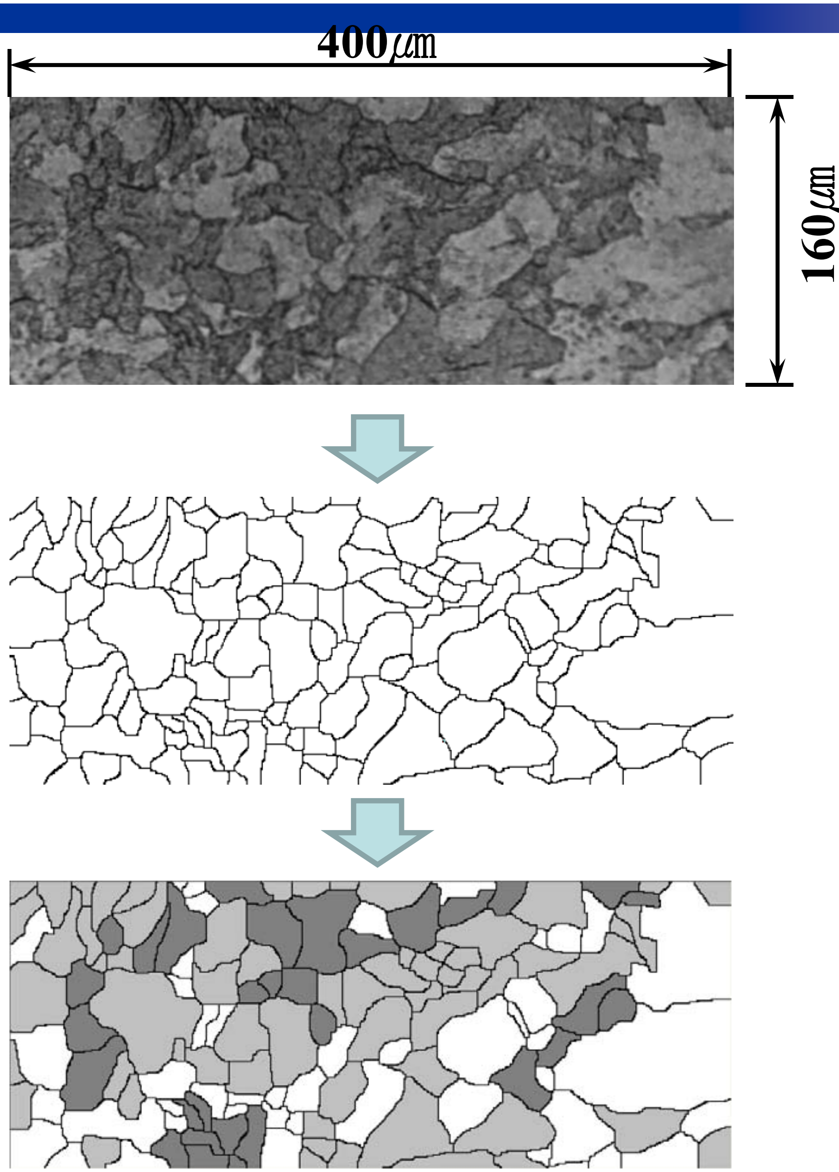

R.W. Margevicius , J. Riedle, P. Gumbsch (1999). "Fracture toughness of polycrystalline tungsten under mode I and mixed mode I/II loading", Materials Science and Engineering A, p197-209

-From the tungsten microstructure morphology in the above paper, digitalization process has been gone through to extract grain boundary shape.

-With the assumption that grains are consist of 3 different orientation and GB to form a microstructure, grain types are assigned to grain region.

DETERMINISTIC FINITE ELEMENT EQUATIONS

- LaGrangian Kinetics Description

$$\int_V \mathbf{s} : \delta\mathbf{F} dV - \int_{S_{int}} \mathbf{T} \cdot \delta\boldsymbol{\Delta}\, dS = \int_{S_{ext}} \mathbf{T} \cdot \delta\mathbf{u} dS - \int_V \rho \frac{\partial^2 \mathbf{u}}{\partial t^2} \cdot \delta\mathbf{u}\, dV,$$

- Finite Element Descretization

$$\mathbf{M}\,\ddot{\mathbf{u}} = -\mathbf{R}$$

- Solution of Equations (Newmark β -Method)

$$\left.\begin{aligned} \ddot{\mathbf{u}}^{n+1} &= -\mathbf{M}^{-1}\mathbf{R}^n \\ \dot{\mathbf{u}}^{n+1} &= \dot{\mathbf{u}}^n + \frac{1}{2}\Delta t_n \left(\ddot{\mathbf{u}}^{n+1} + \ddot{\mathbf{u}}^n \right) \\ \mathbf{u}^{n+1} &= \mathbf{u}^n + \Delta t_n \dot{\mathbf{u}}^n + \frac{1}{2}\left(\Delta t_n\right)^2 \ddot{\mathbf{u}}^n \end{aligned}\right\}$$

PERCENTAGE OF EACH PHASES

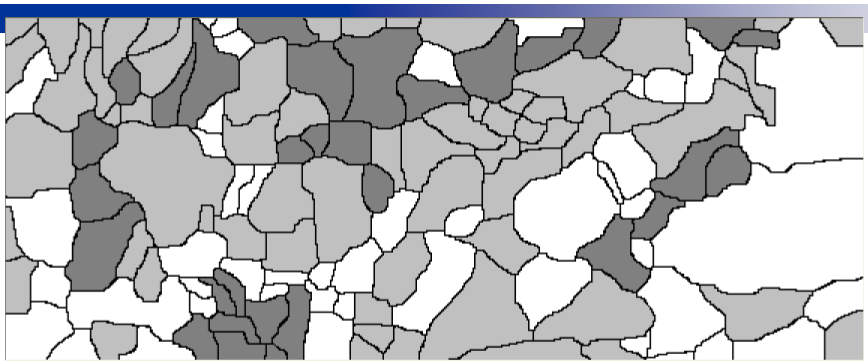

Type	Percentages by Area
GB	7.53 %
Phase1	17.41 %
Phase2	40.43 %
Phase3	34.63 %

For each cases, three different GB properties are applied.

→ Maximum Tensile strength that is

1. **Larger than that of grains**
2. **Same as that of grains**
3. **Smaller than that of grains**

FRAMEWORK

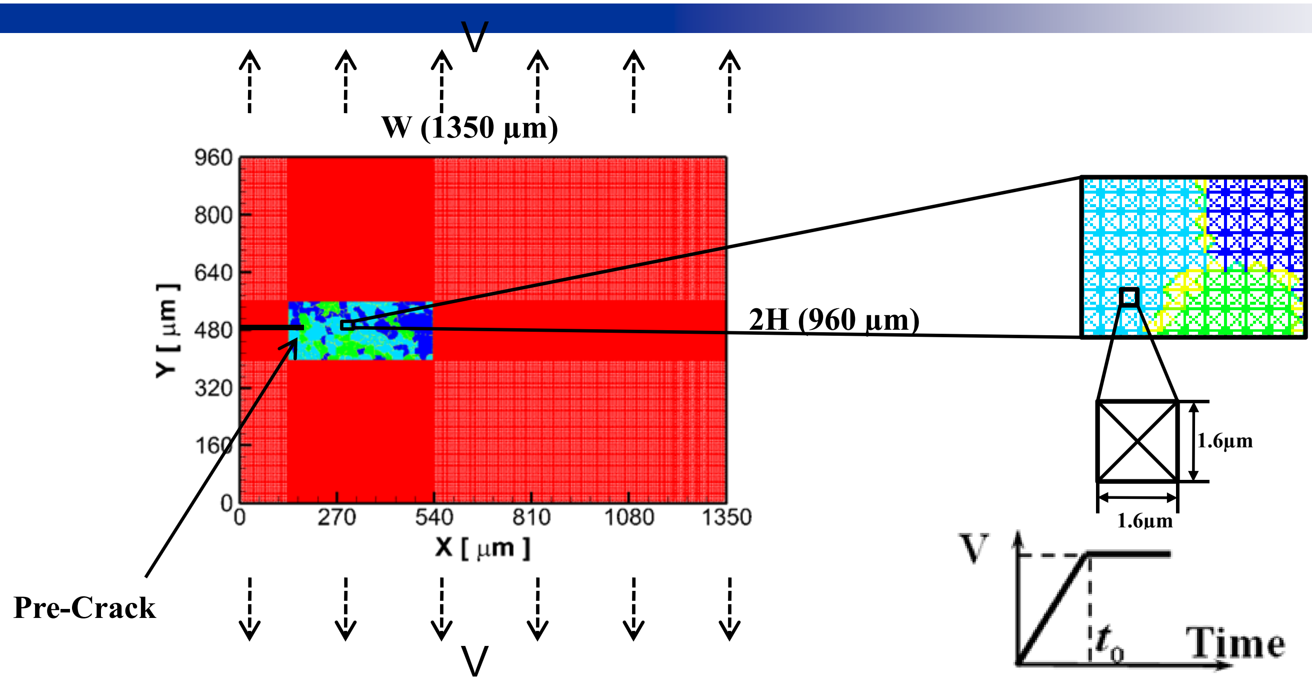

→ All cohesive surfaces serve as potential crack paths.

→ FE meshes are uniformly structured with "cross-triangle" elements to give maximum flexibility for resolving crack extensions and arbitrary fracture patterns.

→ Center-cracked tungsten specimens under tensile loading.

→Initial crack : 20 µm

→ The boundary velocity V (1m/s) is imposed with a linear ramp from zero to V in the initial phase of loading.

→ The specimen is stress free and at rest initially.

COMPARISON FOR COHESIVE ENERGY DISSIPATION

When T = 155 nsec

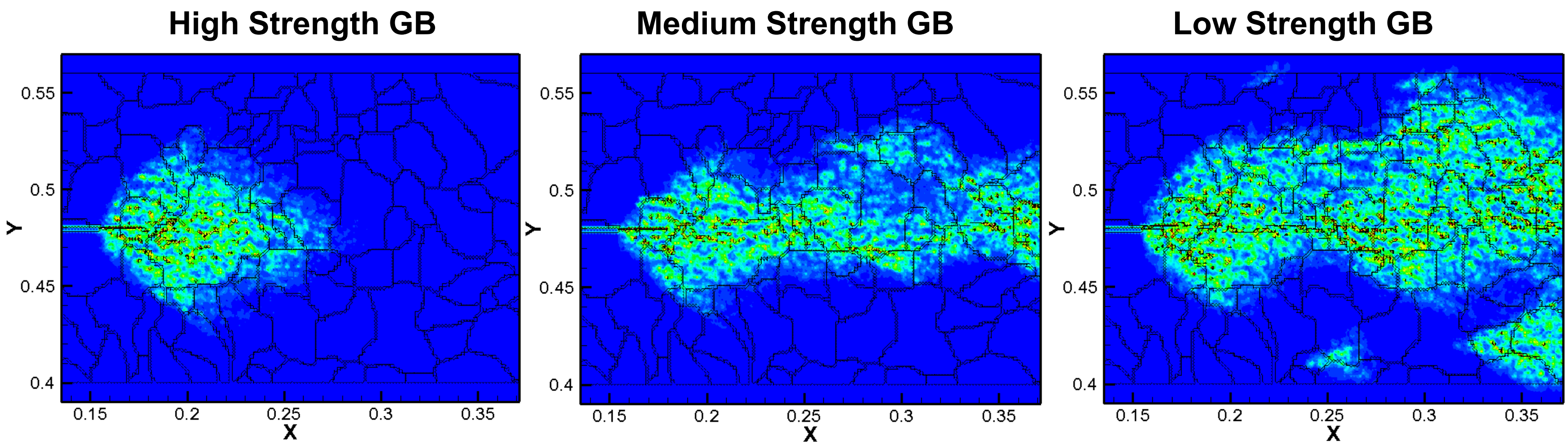

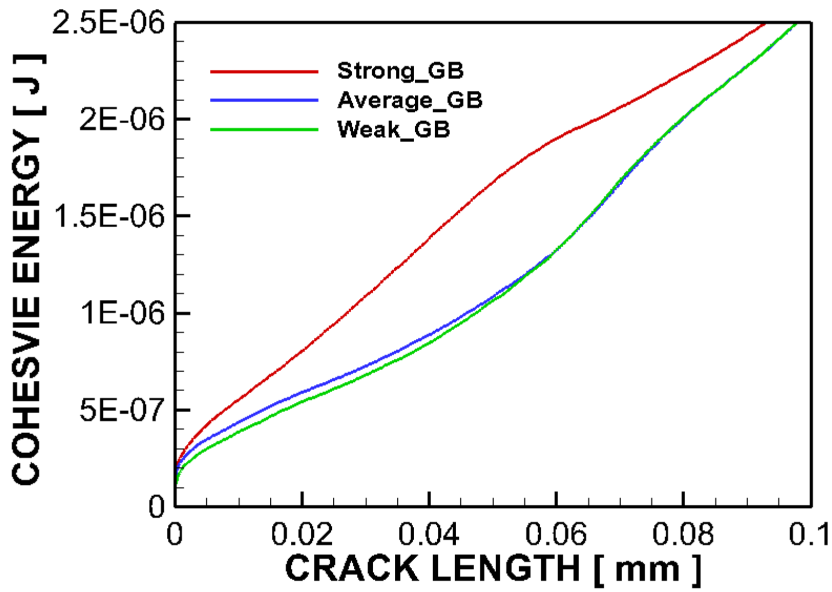

COMPARISON FOR CRACK PROPAGATION DIRECTION

When t = 155 nsec

High Strength GB

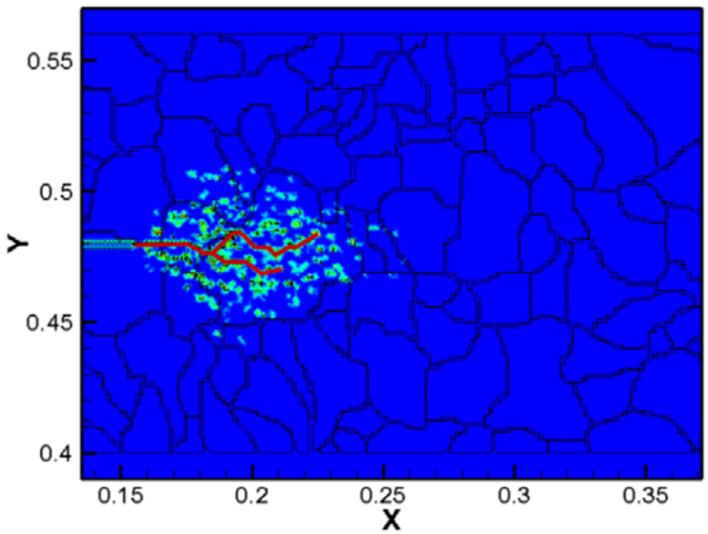

Medium Strength GB

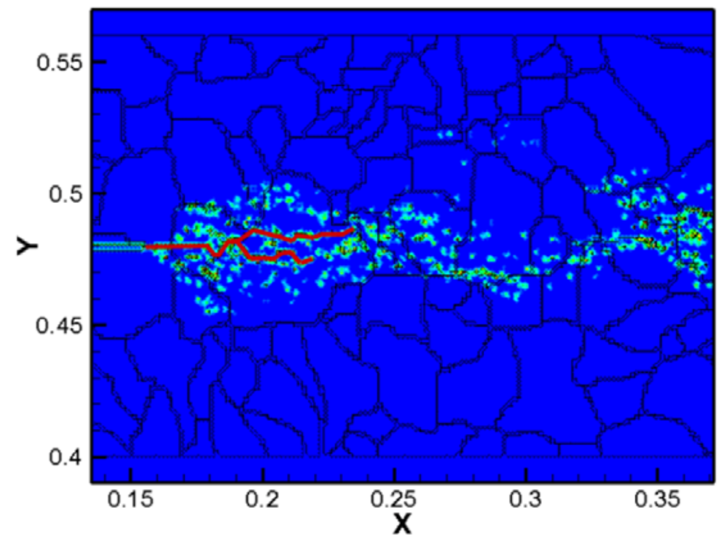

Low Strength GB

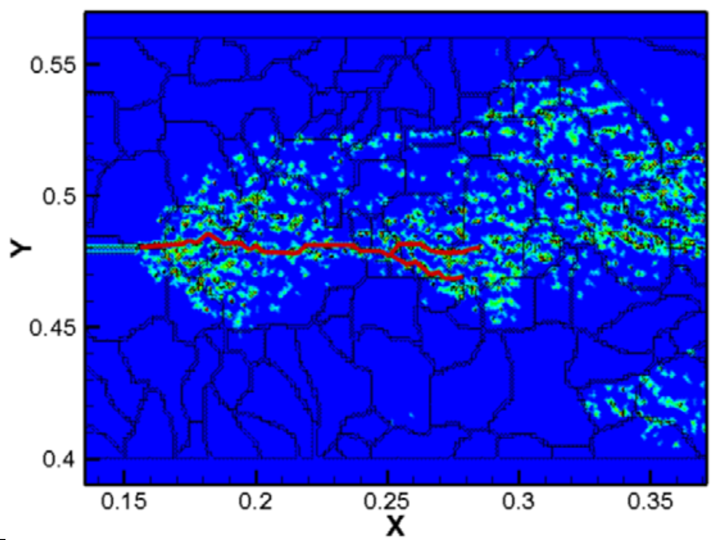

COMPARISON OF PRIMARY CRACK AND MICROCRACKS

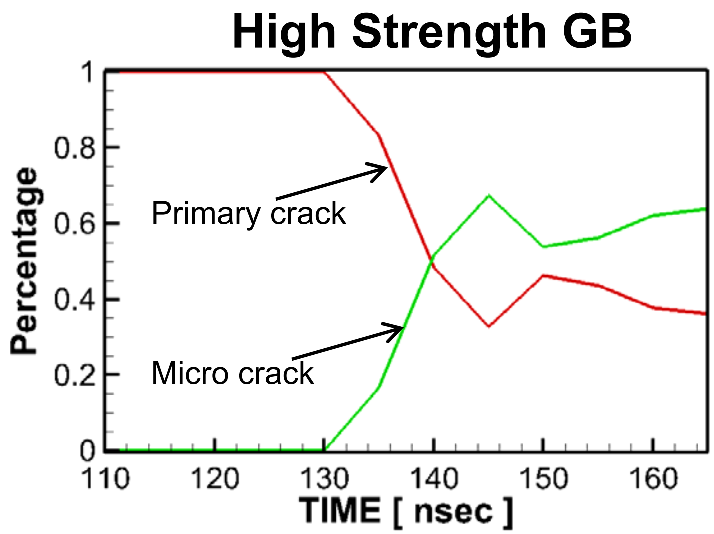

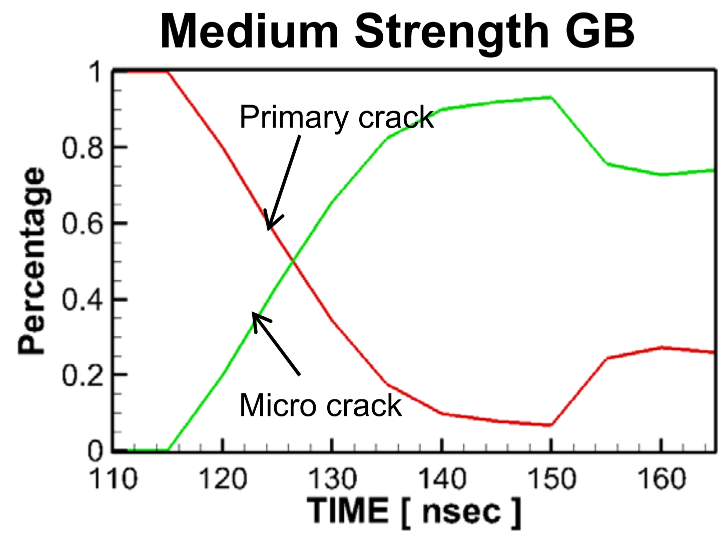

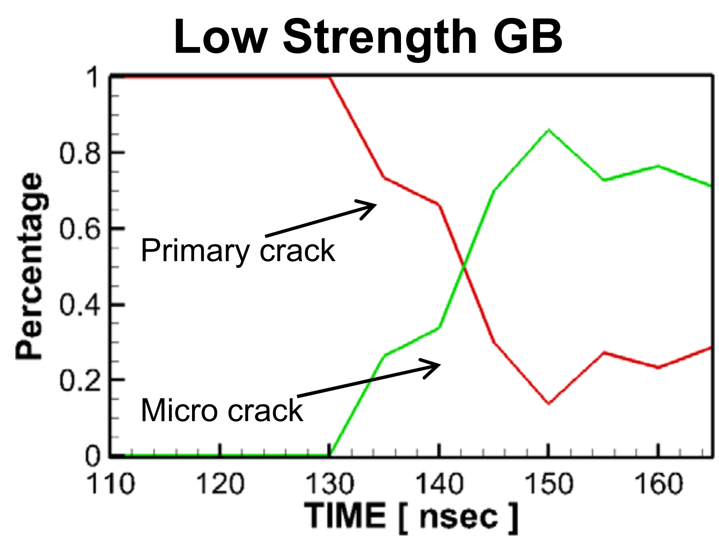

THE RELATION BETWEEN ENERGY DISSIPATION VS CRACK DENSITY

Therefore, $\Phi \cdot \Delta \cdot \frac{(a \times b)}{h^2} \cdot C$ can be explained as energy dissipation per unit crack length or crack density. C is a constant.

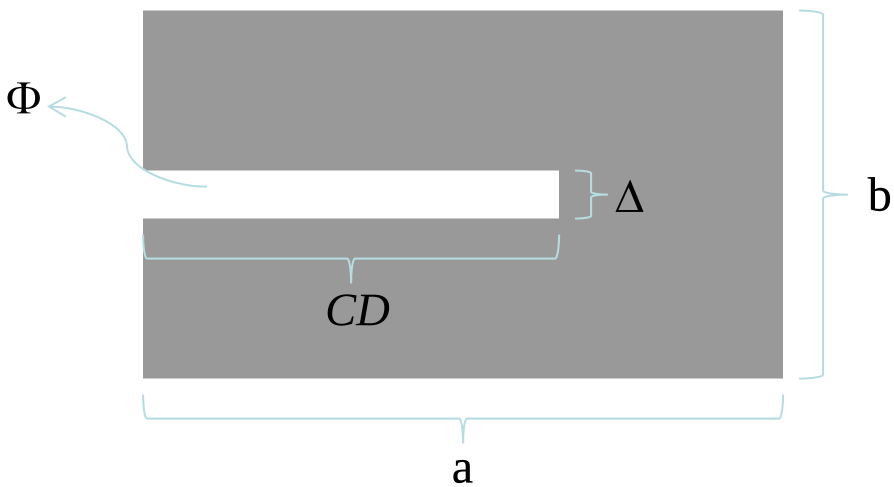

In our case of simulation, C = 12.5 $\quad \mathrm{CE} = 12.5 \cdot \Phi \cdot \Delta \cdot \frac{(\mathrm{a} \times \mathrm{b})}{\mathrm{h}^2} \cdot CD$

By substituting the equation $\Delta = \frac{2 \cdot \Phi}{\mathrm{T}_{\mathrm{max}}}$ to the above equation,

we obtained a relation of $\mathrm{CE} = 25 \cdot \frac{\Phi^2 \cdot (a \times b)}{\mathrm{T}_{\mathrm{max}} \cdot h^2} \cdot CD$

THE RELATION BETWEEN ENERGY DISSIPATION VS CRACK DENSITY

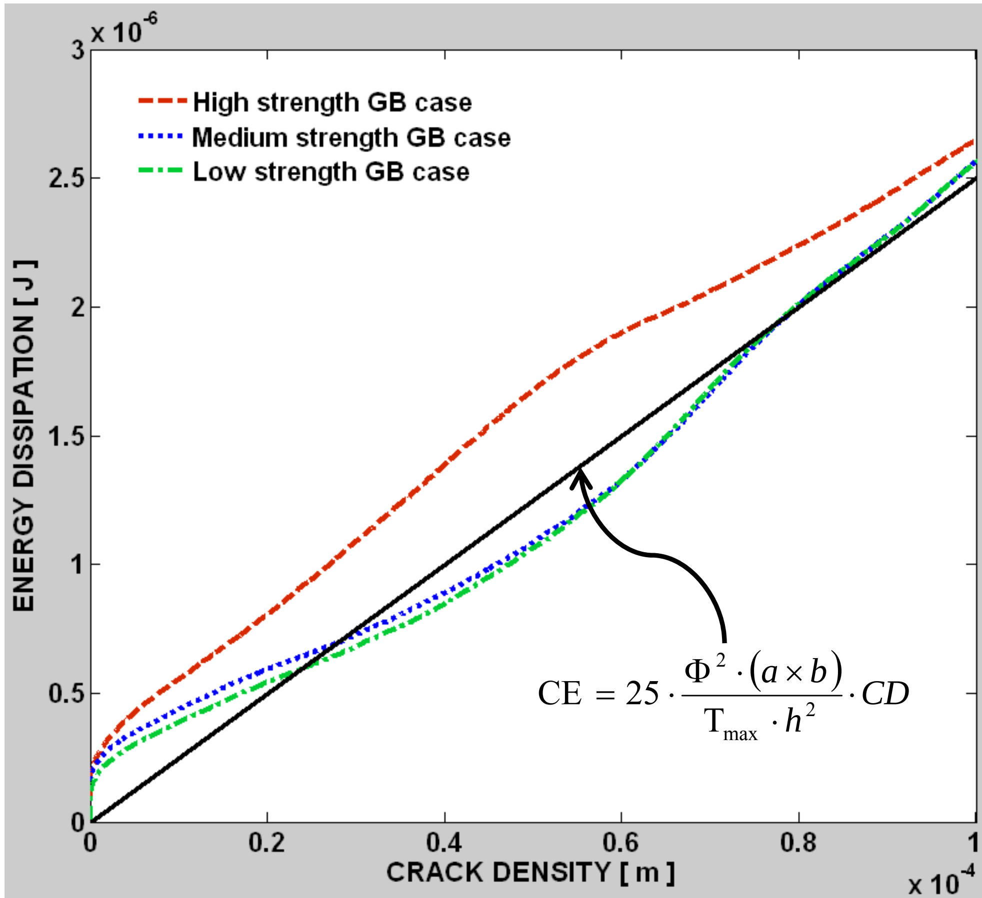

CONCLUSIONS

- Analyses demonstrate that the failure of a tungsten involves inter-granular cracks, intra-granular cracks, and significant microcracking.

- By applying different properties of GBs, plots of cohesive energy dissipation display various patterns of energy release. Property of ductility and brittleness are known as temperature dependent, however, the findings in this study indicates that the tungsten microstrucutural failure can have both ductile and brittle pattern of failure decided also by property of GBs. (GBs have 7.53% by volume)

- The level of microcracking goes greater in the interfaces of grains as strength of GBs becomes lower.

- A significant microcracking occurs during failure. Surface energy study in this research indicates m value to be around 14 for such microstructure with no time dependent. This finding can contribute to predict the level of microcrack over primary crack at other time frames.

- In literature, continuum and analytical fracture mechanics work usually neglects contribution of GBs to overall microstructural fracture strength. The findings in this work indicate property of GB act major role in crack propagation pattern as well as crack initiation time.